NTNU – Trondheim
Norwegian University of
Science and Technology

Control of VSC During Unsymmetrical AC Faults in Offshore Wind Farms

Henrik Kirkeby

Master of Energy and Environmental Engineering
Submission date: June 2013
Supervisor: Kjetil Uhlen, ELKRAFT
Co-supervisor: Kamran Sharifabadi, Statoil ASA

Norwegian University of Science and Technology
Department of Electric Power Engineering

Preface

This master thesis is the work required for the completion of the Energy and Environment MSc program, with specialization in electrical power engineering, and it is weighted with 30 ECTS. It was set up in collaboration between the Norwegian University of Science and Technology (NTNU), SINTEF Energy AS and Statoil ASA, with Kjetil Uhlen, Atle Rygg Årdal and Kamran Sharifabadi as supervisors.

Acknowledgments

I want to thank my Lord Jesus Christ for that I can write this report and finish my masters's degree here at NTNU. Working on my master thesis this past six months have, at times, been quite challenging. It is then good to look back and see that while it was difficult for me to get to the end of this semester, it probably did me well. I do believe he has enabled me to learn and grow this semester, also in areas in life unrelated to electrical power engineering.

There are many people to thank for that I have something to deliver at the end of this semester, most notably Atle Rygg Årdal, who has endured many, long and repetitive meetings with me, and still managed to give good advice and constructive answers to questions I perhaps should have known the answer to before I came to see him. Kjetil Uhlen, my main supervisor, have always been pleasant, helpful and forthcoming when i met him, and he has been inspiring by showing an actual interest in the work I have been doing. Kamran Sharifabadi have been helpful and full of good initiatives, and I am sorry that I have not taken more use of his offer to contact him. Jon Are Wold Suul was the first person to point out some general difficulties with my simulation model, and was very helpful when I needed further direction in modelling the control system in this exercise. I am also grateful that Sverre Gjerde have been providing tips for my simulation model.

Even if I cound have done the bulk of my work from home by using VPN, I continued to work at the office, because I would not want to miss out an epic semester with card games, lunch breaks and good conversations with my class mates at the office.

I also want to thank the guys in my bible study group for praying for me, that they showed an interest in my work and by just being perfect.

Abstract

This master thesis has analyzed the effects of unbalanced faults in the AC grid of an offshore wind farm. The wind farm is connected to shore with a Voltage Source Converter (VSC) HVDC link, and the wind turbine generators employs VSC technology in full scale converters. The offshore wind farm have been modelled in Matlab SIMULINK, and there have been performed different short circuit simulations at various places in the offshore AC grid. A control method designed to control positive and negative sequence currents in parallel have been tested and compared to a standard control system during these short circuit simulations. The theory behind the modelled negative sequence current controller is that it can be used to control active power oscillations, thus limiting DC voltage oscillations caused by this pheonmena.

The simulation model built in Matlab SIMULINK could be further optimized, and many challenges were faced to obtain a functioning and stable control system. Due to this, the negative sequence current controller is only enabled in the wind turbine converter, and not in the HVDC link offshore converter. Still it should be able to dampen out the oscillations in the HVDC link. The results obtained from the simulations show that in general the negative sequence current controller does not improve the oscillations on the HVDC link DC voltage significantly. When it is enabled, it performs worse than the standard controller during a three phase fault, which in theory should give equal results with the two control systems. This means that the problem is probably not the theory of the negative sequnce current controller, but rather the implementation of the controller in the modelled system. It is therefore recommended further work to obtain a more credible simulation model with better tuned controller parameters.

This thesis has resulted in a Matlab SIMULINK model based on the NOWITECH reference turbine, and there are many possibilities for further research on the reference turbine, as well as general research on control of offshore wind farms during fault ride throughs and other transient conditions. A brief overview over challenges and pitfalls when building a large simulation model in Matlab SIMULINK is available in Appendix A, this is very much recommended for students undertaking their first large project in Matlab SIMULINK.

Sammendrag

Denne masteroppgaven har analysert effektene av usymmetriske feil i et vekselstrømsnett i en havvindspark. Havvindsparken er koblet til land via en spenningsomformerbasert HVDC link, og vindturbingeneratorene bruker også fullskala frekvensomformere. Ved å modelere havvindsparken i Matlab SIMULINK, og ved å utføre ulike kortslutningssimuleringer forskjellige steder i vekselsstrømsnettet til havs, så har en kontrollmetode som kan kontrollere positiv og negativ sekvensstrøm blitt designet og sammenlignet med et standard kontrollsystem. Teorien bak den modellerte negativsekvens strømkontrolleren er at den kan bli brukt til å kontrollere oscillasjoner i aktiv effekt som er til stede under ubalanserte nettilstander, og dermed til å begrense DC spenningsoscillasjonene som kommer fra dette fenomenet.

Simuleringsmodellen som er satt sammen i Matlab SIMULINK har forbedringspotensiale med tanke på innstilling av kontrollerparametre, og det viste seg å være en stor utfordring å sette sammen et fungerende og stabilt kontrollsystem. På grunn av dette er det kun brukt negativsekvens strømkontroller i vindturbinomformeren. Resultatene fra simuleringene viser at negativssekvensstrømkontrolleren stort sett ikke demper svingningene i DC spenningen i HVDC linken. Ved test av en trefase feil i simuleringsmodellen gir negativssekvensstrømkontrolleren et svakere resultat enn standardkontrolleren, selv om dette i teorien skulle føre til samme resultat for de to kontrollsystemene. Dette betyr at problemet sannsynligvis ikke er teorien rundt negativssekvensstrømkontrolleren, men heller implementeringen av denne kontrolleren i simuleringsmodellen. Det er derfor anbefalt videre arbeid for å sette i stand en mer troverdig simuleringsmodell med bedre konfigurerte kontrollparametre.

Masteroppgaven har ikke bare denne rapporten som resultat, men også simuleringsmodellen brukt til å utføre kortslutningsmodelleringene. Denne modellen er basert på NOWITECH sin referanseturbin, og det er mange muligheter videre for å gjøre mer forskning på referanseturbinen og mer generell forskning på havvindsparker under forskjellige transiente forløp som kortslutninger i nettet på land. Videre inkluderer denne masteroppgaven en oversikt over utfordringer og fallgruver når man skal sette sammen en større simuleringsmodell i Matlab SIMULINK. Denne finnes i Appendix A, og den er sterkt anbefalt for studenter som for første gang skal utføre et større prosjekt i Matlab SIMULINK.

Table of Contents

List of Figures

Cover Photo: Andy S-D, Flat Calm. www.flickr.com 2006.

List of abbreviations

- Back to back - b2b
- GS - Grid Side
- IGBT - Insulated-Gate Bipolar Transistor
- LCC - Line Commutated Converter
- LP filter - Low Pass Filter
- MMC - Multi Modular Converter
- NSC - Negative Sequence Current Controller
- NSCC - Negative Sequence Current Controller
- PI controller - Proportional + Integral controller
- PID controller - Proportional + Integral + Derivative Controller
- PLL - Phase Lock Loop
- PMSG - Permanent Magnet Synchrounous Generator
- PR controller - Proportional Resonant controller
- PS - Park Side
- PSC - Positive Sequence Current
- PSCC - Positive Sequence Current Controller
- SOGI-QSG - Second Order Generalized Integrator - Quadrature Signal Generator
- SRF - Synchronous Rotating Reference Frame
- VCC - Vector Current Control
- VSC - Voltage Source Converter
- WPP - Wind Power Plant
- WTG - Wind Turbine Generator

1 Introduction

Renewable energy has been an increasingly important source of energy in the world the last couple of years. Wind in particular has grown as a source of electricity generation, due to benefits such as zero emissions during generation, free fuel, non dependence on foreign resources such as oil, and recently a more matured technology. Wind energy has also been widely implemented in the energy sector due to its abundance most places in the world and because of proven technology. In the later years offshore wind has gained momentum in North West Europe, with countries such as UK, Denmark, Germany and the Netherlands installing huge amounts of offshore wind farms. Global Wind Energy Council projects that in 2020, the EU will have installed 40 GW of offshore wind [1]. The reason for this popularity is due to among other things, stronger and more steady wind offshore, less noise and visual pollution from the turbines and more available space. Due to these reasons, an offshore wind farm will have a higher capacity factor than an onshore wind farm, resulting in a better return on the investment. The downside of offshore wind is the massive upfront costs, and the high maintenance costs. Moreover, area suitable for near shore wind is quite limited, and new wind farms are being built further and further offshore, greatly increasing the investment costs.

Since offshore wind is being built further and further offshore, AC transmission becomes challenging. The capacitive charging current limits the transmitted power through the cable, so that for distances over approximately 90 km, it would be cheaper to install an HVDC system rather than an AC system. [2] Voltage Source Converter technology has become the prefered HVDC techonology due to its black start capabilities, as well as the possibility to connect to a weak grid. Line Commutated Converters (LCC) HVDC tecnology on the other hand, require grid synchronization voltage, as well as a Short Circuit Ratio over 2 to connect to a system. This means that it can only connect to a system that has an equivalent reactance that is low, while a WPP often has a large reactance, which makes LCC unsuitable for WPPs. LCC also has greater demands for filters and reactive power compensation. This increases the required area, which results in higher costs, due to the high construction costs offshore. VSC is a relatively young technology, the first commercial project was construced in 1997 when ABB introduced its HVDC Light product [3]. The principle of operations remains the same today, allthough the converters have become much more complex with the introduction of cascaded two level converters by ABB and Multi Modular Converters (MMCs) by Siemens called HVDC PLUS and a similar product from Alstom. This project will not focus on the MMC topology, but rather

on the basic concept as introduced by ABB, namely the two level converter.

Wind Power Plants (WPP) have several fundamental differences than ordinary power plants. Due to the power electronics the WPPs will have a significantly lower short circuit current and by default there is virtually no inertia in the system. New control methods are introduced to ensure that WPPs can cope with the various grid code requirements, so that they can stay connected during faults and provide reactive power compensation to the grid. The power electronics however, makes the system vulnerable to overcurrents and overvoltages as they could destroy the converters. Control systems can be designed so that the converters limit the maximum current that will pass through. For unbalanced network conditions, theory indicates that converter control systems can be designed to control both positive and negative sequence currents in the system in order to avoid DC voltage oscillations on the HVDC link and in the Wind Turbine Generators (WTGs).
This thesis will study:

- How will various faults in the offshore AC grid affect the offshore wind farm?
- Could there be an improvement in how the system is able to cope with faults by introducing negative sequence current controllers (NSCC) in the control system?
- What are the challenges in implementing these controllers and creating a simulation model to test this hypothesis?

This will be studied by creating a model of an offshore WPP in Matlab SIMULINK, and simulating various short circuits at different locations. Chapter 2 will give a short introduction to NOWITECH and the reference turbine. Chapter 3 will list background theory regarding VSC control, as well as information regarding unbalanced faults and positive and negative sequence analysis. Chapter 4 will present the simulated system assumed to consist of turbines specified as the NOWITECH RT, with components and control philosophy, including tests on the individual controllers. Chapter 5 will give the results of a full simulation run in order to explain what is happening during a fault in the offshore AC grid, and how the simulation model is working. Then the simulation results are presented, most of the figures from the simulations have not been included and can be found in the Appendix E. Chapter 6 discuss the results from the previous chapter, and suggest improvements. Chapter 7 will give a conclusion to this project and recommendation for further work.

This project will only deal with faults in the AC network, and does therefore not concern topics such as DC choppers and HVDC breakers. Due to the limited time available, only faults in the offshore AC grid have been considered, and not in the onshore grid to test fault ride through requirements and so forth. The modelled system is also very basic, and contains few filters and no AC breakers. The modelled wind farm have, for most of the simulations, been aggregated into one turbine to keep simulation time as low as possible.

2 NOWITECH

The Norwegian Research Center for Offshore Wind Technology (NOWITECH) project is a joint research project started in 2009 and hosted by SINTEF, which aims to lay the foundation for industry value creation and cost effective offshore wind farms through pre-competitive research [4]. The NOWITECH project focuses on a large range of activities, the topic of this master thesis will be on grid connection and system integration of large offshore wind farms.

2.1 Reference Turbine

The NOWITECH project have designed a reference turbine, which is a 10 MW offshore wind turbine model developed for testing out novel technologies and establishing a industry base model. Moreover, industry actors are reluctant to hand over their wind turbine models, so this reference turbine will also suffice as a model for academic work and research, such as this master thesis.

The wind turbine rotor has a diameter of 141 m, and the turbine has rated production for wind speeds higher than 13 m/s [5]. The tower is chosen to be a bottom fixed four legged lattice structure. The generator used in the turbine is a direct drive Permanent Magnet Syncronous Generator (PMSG) with a full scale converter. The maximum rotational speed is 13.5 rpm, and the number of pole pairs in the turbine is in set to 250. Other turbine data is listed in figure 1, for a more comprehensive list consult Appendix A.

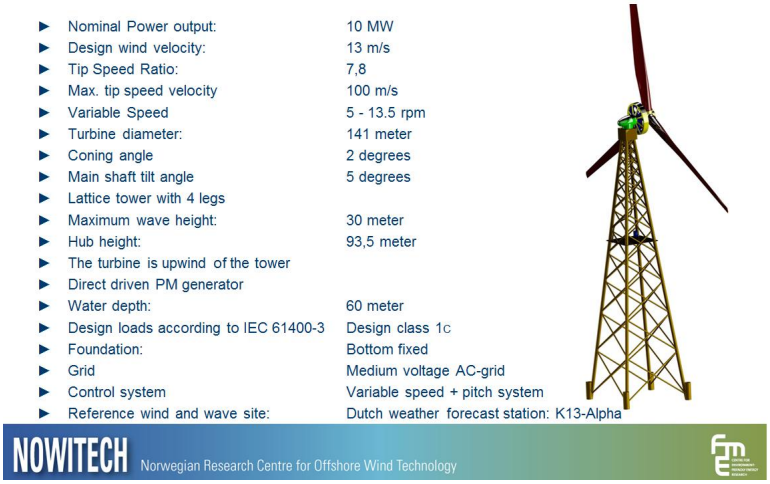

Figure 1: Reference Turbine Data

The planned converter layout to be used in the WTG is shown in figure 2. This is a three level back to back (b2b) AC/DC converter. The converter is neutral point clamped with diodes. In addition to the filters in the figure, the converter also employs 3^{rd} harmonic injection and two DC choppers for effective network control.

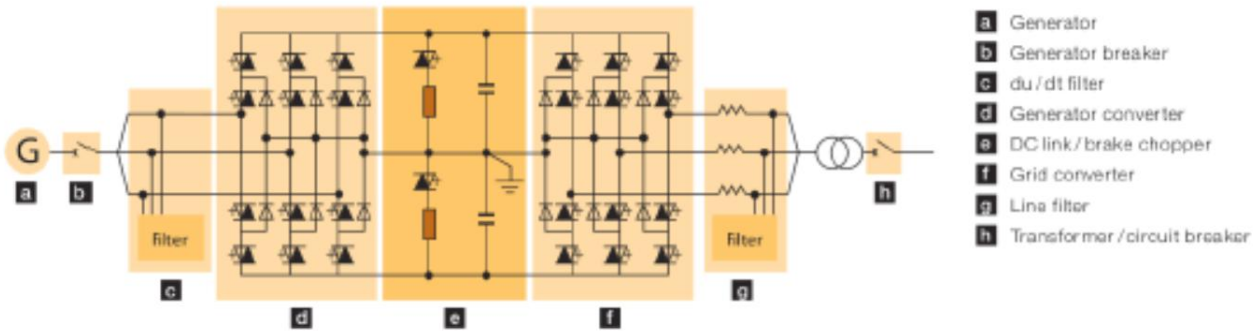

Figure 2: Converter Layout

The turbine is implemented in the SIMULINK model used in this master for running the required simulations, so that not only the general behaviour of the offshore grid can be studied, but also the response on the WTG. The motivation for looking at the specific turbine is to see how the turbine responds to faults in the grid with a given control scheme, and perhaps in later simulations, to see whether performance is satisfactory with regards to the grid code requirements (GCR). The NOWITECH reference turbine is still a work in progress, and not all aspects of the turbine have yet been determined. The goal of this master is not to set these parameters, but rather to start to examine some of the different challenges and possibilities in terms of control and wind farm layout. The simulation model including the NOWITECH turbine, can be used for further testing and to research these topics more extensively.

3 Background Theory

This chapter will deal with the various control methods for VSC used in this master thesis, as well as some background theory on unbalanced faults and sequence analysis during faults. Acompanying the background theory there will be a simplified figure of the model, indicating which part of the model the presented theory is valid for. The whole system is shown below in figure 3, and is presented in detail in section 4.1.

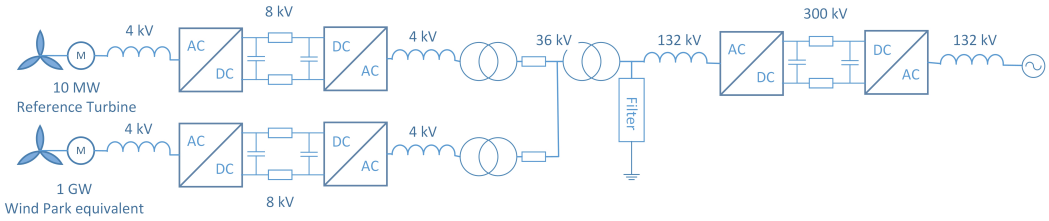

Figure 3: Topology of the Offshore Wind Farm

3.1 VSC Control

This section will present the all parts of the standard positive sequence control scheme used for the simulation model, with the exception of the WTG controll system presented in chapter 3.2.

3.1.1 Vector Current Controll

The inner current controllers in this project have been implemented as Vector Current Control (VCC), as presented in [6] and [7].

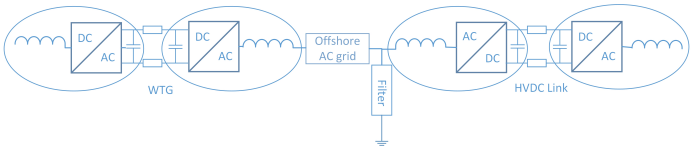

Figure 4: Locations Relevant for Vector Current Control

A VSC can be modelled as shown in figure 5, where the relation between U_{DC} and v_c is:

$$v_c = m_a \frac{U_{DC}}{2} \tag{3.1}$$

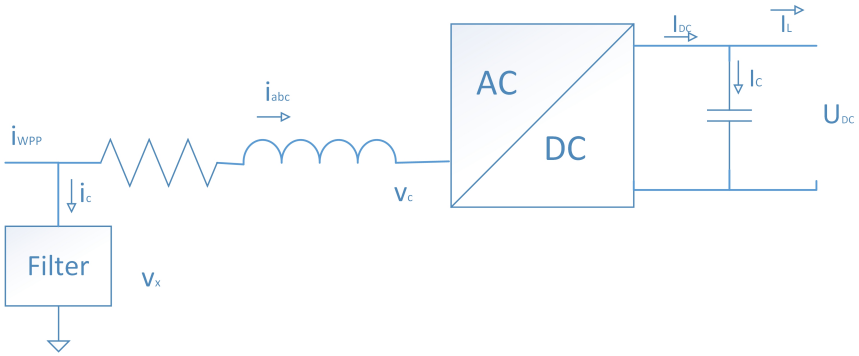

Figure 5: Simple VSC model

where m_a is the modulation index. If one has a passive network, with a load Z_L, one can control the desired voltage v_x by using the voltage division relation of v_c and v_x, making the a network voltage controller with controll objective:

$$v_x = \frac{Z_L}{Z_L + R + j\omega L} m_a \frac{U_{DC}}{2} \tag{3.2}$$

This project however, wil only contain active networks. To analyze these, Kirchoffs Voltage Law is applied across the inductor, which results in:

$$v_x - v_c = L\frac{di}{dt} + iR \tag{3.3}$$

Should one consider a synchronous rotating reference frame (SRF) in a three phase AC system where the d axis is aligned to v_a, we could apply the voltage invariant Park transformation and write this as:

$$\begin{bmatrix} v_{c,d} \\ v_{c,q} \end{bmatrix} = \begin{bmatrix} v_{x,d} \\ v_{x,q} \end{bmatrix} - \begin{bmatrix} R & -Lw \\ Lw & R \end{bmatrix} \begin{bmatrix} i_d \\ i_q \end{bmatrix} - L\frac{di}{dt} \tag{3.4}$$

In this reference frame, power would be given by:

$$S = \frac{3}{2}(v_{x,d} + jv_{x,q})(i_d - ji_q) \tag{3.5}$$

$$P - jQ = \frac{3}{2}(v_{x,d}i_d + v_{x,q}i_q) - j\frac{3}{2}(v_{x,d}i_q - v_{x,q}i_d) \tag{3.6}$$

During steady state balanced conditions, this becomes simplified because

$v_{x,q} = 0$ so:

$$P - jQ = \frac{3}{2} v_{x,d} i_d - j\frac{3}{2} v_{x,d} i_q \tag{3.7}$$

If one considers the converter as a time delay equal to half the switching frequency f_s, then the controller, converter and system can be modelled as in figure 6, where L is reactor inductance, R is reaktor resistance, ω is grid frequency, and:

$$T_s = \frac{1}{2f_s} \tag{3.8}$$

where f_s is switching frequency.

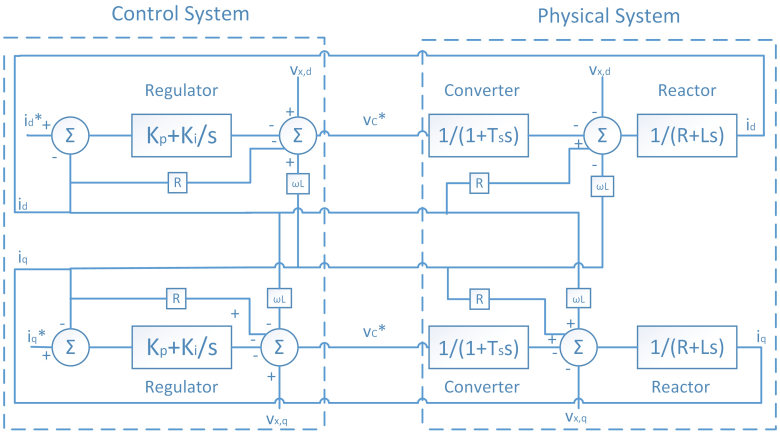

Figure 6: Converter system and control

The current references will be calculated differently depending on the control objectives. During this project, only U_{DC}, Q and v_{AC} will be relevant to control for standard positive sequence current controllers (PSCCs), and so only these outer contol loop variant will be discussed here.

It should be noted that v_c will only be equal to v_c*, which is the output of the VCC, when $U_{dc,pu} = 1$. To avoid this unlinearity in the system, a different control system is proposed for the reference to the PWM module [8]. This is presented in the figure 7

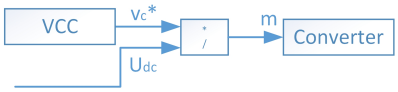

Figure 7: Alternate Control Scheme for v_c*

3.1.2 Control of U_{DC}

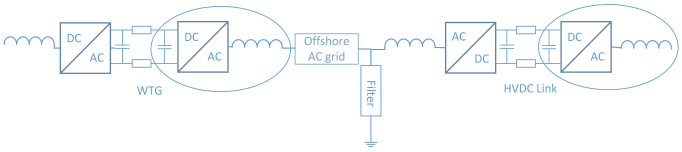

Figure 8: Locations Relevant for Control of U_{DC}

The control of the DC voltage can be analyzed by setting up the power relatation:

$$P_{AC} = P_{DC} + P_{cap} \tag{3.9}$$

$$\frac{3}{2} v_{x,d} i_d + U_{DC} I_{DC} = U_{DC} C \frac{dU_{DC}}{dt} \tag{3.10}$$

Which gives:

$$dU_{DC}/dt = \frac{3v_{x,d}}{2CU_{DC}} (i_d + \frac{2U_{DC}}{3v_{x,d}} I_{DC}) \tag{3.11}$$

This gives after implementing a feed forward term for I_{DC} the outer control loop depicted in figure 9:

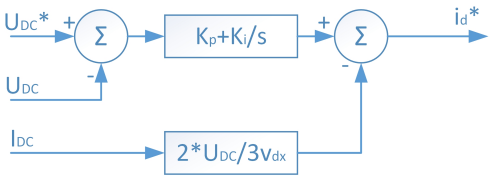

Figure 9: U_{DC} regulating i_d reference block diagram

3.1.3 Control of Q

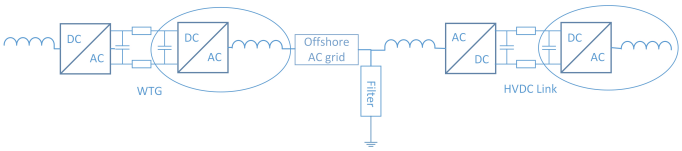

Figure 10: Locations Relevant for Control of Q

From equation 3.7, we get the outer control loop as presented in figure 11:

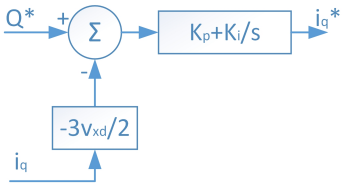

Figure 11: Q regulating i_q reference block diagram

3.1.4 Control of v_{AC}

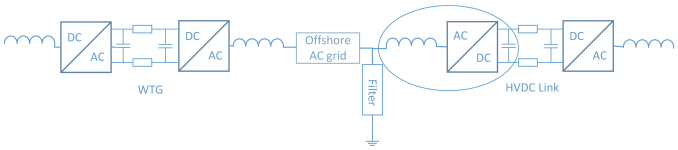

Figure 12: Locations Relevant for Control of v_{AC}

Kirchoffs Current law on figure 5 results in:

$$\begin{bmatrix} i_d \\ i_q \end{bmatrix} = \begin{bmatrix} i_{WPP,d} \\ i_{WPP,q} \end{bmatrix} - \begin{bmatrix} i_{c,d} \\ i_{c,q} \end{bmatrix} \tag{3.12}$$

$$\begin{bmatrix} i_{c,d} \\ i_{c,q} \end{bmatrix} = \begin{bmatrix} 0 & -\omega C_f \\ \omega C_f & 0 \end{bmatrix} + C_f \begin{bmatrix} dv_d/dt \\ dv_q/dt \end{bmatrix} \tag{3.13}$$

Which can be translated to the outer control loop in figure 13:

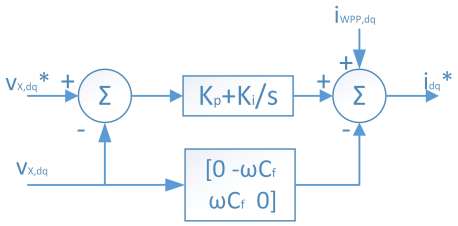

Figure 13: v_{ac} regulating i_{dq} reference block diagram

3.1.5 Positive Sequence Control System Layout

The control objectives presented here can be combined into one control system, that can switch between controlling U_{DC} and Q, and v_d and v_q. This control system is presented in figure 14

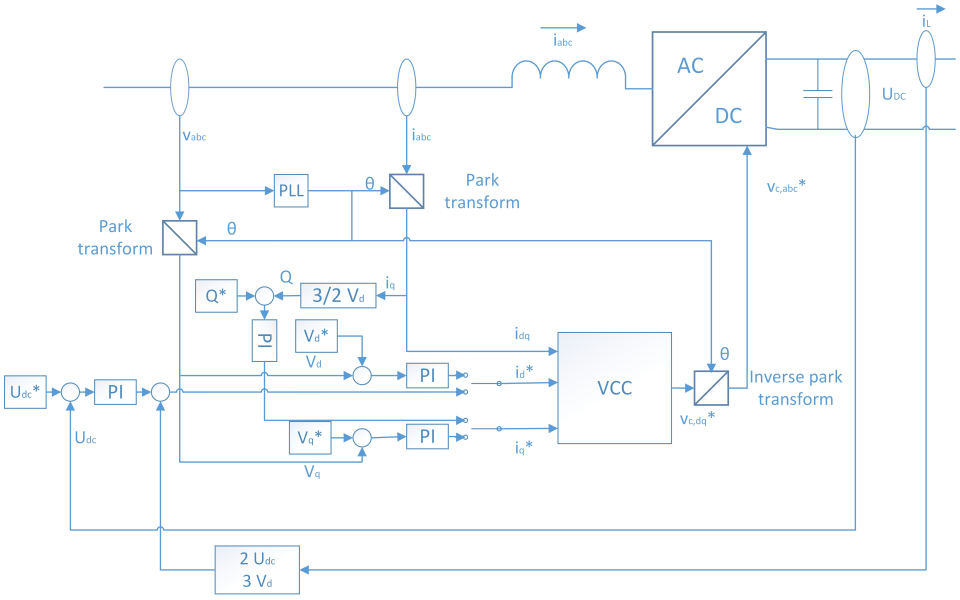

Figure 14: The Control Scheme Applied in the Simulation Model

In addition to the control objectives presented in the previous sections, it is also possible to control power and frequency, and one might add droop control to any of these controllers, so that for example both power and voltage can be controlled by the i_d current reference.

3.2 WTG Modelling and Control

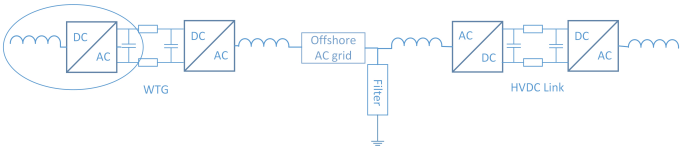

Figure 15: Locations Relevant for Control of the WTG

This subsection will discuss the modelling and control of the WTG with the converter. The generator of the wind turbine is a PMSG, and the generator terminal voltage can be described by the following equations [9]:

$$\begin{aligned} v_{cd} &= R_s i_d - \omega \psi_{sq} + \frac{d\psi_{sd}}{dt} \\ v_{cq} &= R_s i_q - \omega \psi_{sd} + \frac{d\psi_{sq}}{dt} \end{aligned} \tag{3.14}$$

Where the d axis is alligned with the rotor flux ψ_r. The stator flux ψ_{sdq} can be described by:

$$\begin{aligned} \psi_{sd} &= L_{sd} i_d + \Psi_f \\ \psi_{sq} &= L_{sq} i_q \end{aligned} \tag{3.15}$$

Furthermore, the electrical torque can be expressed by:

$$T_e \approx p i_{sq} \Psi_f = J \frac{d\omega_m}{dt} - T_m \tag{3.16}$$

Similar as in figure 6, one can create VCC control for the generator side converter. The references i_d and i_q can be used to control two different parameteres in the generator. The reference turbine is a pitch regulated turbine, so the turbine controls generator speed for wind speeds below rated, and pitching angle for wind speeds above rated. The power extracted from the wind depends on the aerodynamic properties of the rotor described by the power coefficient

$$c_p(\lambda, \beta) = \frac{P_m}{\frac{1}{2}\rho A v^3} \tag{3.17}$$

where: $\lambda = \frac{\omega_m R}{v}$ and β is the pitch angle. For lower wind speeds, β is fixed, and there exists a optimal λ that maximizes the power coefficient. [10]

By using equation 3.16, one sees that by varying the electrical power that goes out of the wind turbine, one can vary the speed, and thereby λ. Since electrical torque is proportional to i_q as stated in equation 3.16 and power is proportional to torque,the current reference i_q can be generated by using a PI controller on the difference of the electrical power P_e and the reference for the electrical power. The reference for the electrical power is determined by a lookup table that provides a relation between generator speed and ideal power output. This shown in figure 16. i_d^* is set to zero to minimize maximum current through the stator, but can also be specified in order to minimize losses in the WTG.

For wind speeds above rated, the rotor mechanical power is potentially larger than the generator rating, so power output and reference power is compared and fed through a PI controller to control the pitch angle to effectively limit mechanical power output. The output of this PI controller has a rate saturation to account for the finite time required to pitch the WT blades.

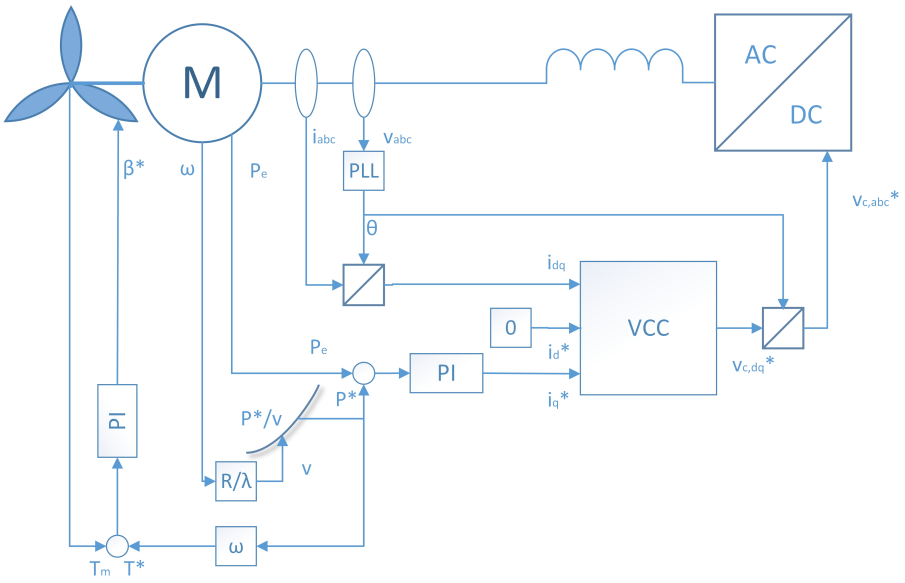

Figure 16: The WTG Control Scheme Applied in the Simulation Model

3.3 Clarke - and Park Transformation

The voltage and current is transformed from abc to $\alpha\beta$ and dq variables in the converter controlsystem by using the following verion of the Clarke - and Park Transformation:

$$\begin{bmatrix} v_\alpha \\ v_\beta \end{bmatrix} = \frac{2}{3} \begin{bmatrix} 1 & -\frac{1}{2} & -\frac{1}{2} \\ 0 & \frac{\sqrt{3}}{2} & -\frac{\sqrt{3}}{2} \end{bmatrix} \begin{bmatrix} v_a \\ v_b \\ v_c \end{bmatrix} \tag{3.18}$$

$$\begin{bmatrix} v_a \\ v_b \\ v_c \end{bmatrix} = \begin{bmatrix} 1 & 0 \\ -\frac{1}{2} & \frac{\sqrt{3}}{2} \\ -\frac{1}{2} & -\frac{\sqrt{3}}{2} \end{bmatrix} \begin{bmatrix} v_\alpha \\ v_\beta \end{bmatrix} \tag{3.19}$$

$$\begin{bmatrix} v_d \\ v_q \end{bmatrix} = \begin{bmatrix} sin\theta & cos\theta \\ cos\theta & -sin\theta \end{bmatrix} \begin{bmatrix} v_\alpha \\ v_\beta \end{bmatrix} \tag{3.20}$$

$$\begin{bmatrix} v_\alpha \\ v_\beta \end{bmatrix} = \begin{bmatrix} -sin\theta & cos\theta \\ cos\theta & sin\theta \end{bmatrix} \begin{bmatrix} v_d \\ v_q \end{bmatrix} \tag{3.21}$$

3.4 Faults

This subsection will explain the effect of unbalanced faults on the converter controller, before presenting the background theory for creating a NSCC that can control active power oscillations to be zero.

3.4.1 Fault Types and the Effect on the Converter Controller

There are four types of faults that occur in an three phase AC system. There are Single Line to Ground (SLG) faults; Double Line (DL) faults; Double Line to Ground (DLG) faults; and Tripple Line to Ground (3PG) faults. SLG, DL and DLG type of faults will lead to an unbalanced system, where voltages in the healthy lines will be higher than in the faulted ones. [11] states that when neglecting the zero sequence component, which often is blocked out by the transformers, the voltages can be decomposed into positive and negative sequence components. When transforming voltages to the Synchronous Rotating reference Frame (SRF), the negative sequence components will be in a reference frame rotating at the speed of $-\omega$, while the positive components will be in SRF rotating at ω. the transfer function from the positive SRF to the negative will then be:

$$H_{+to-} = e^{-j2\omega t} \tag{3.22}$$

When performing the Park transformation, we can see that the negative sequence components that will cause oscillations at 2ω, or 100 Hz frequency, in the system voltage. This will therefore give power oscillations with 100 Hz frequency through the converters. This is problematic because the oscillations can exceed the ratings of the converters, and in the worst case destroy them. Oscillations may also be sent out to the onshore grid, which is undesirable.

3.4.2 Negative Sequence Current Controller References

The power through the converters [11] can be expressed by:

$$\begin{aligned} S &= v * i^* \\ &= (v^+ + v^-)(i^{+*} + i^{-*}) \\ &= P_0 + P_{cos2\omega} cos2\omega + P_{sin2\omega} sin2\omega + Q_0 + Q_{cos2\omega} cos2\omega + Q_{sin2\omega} sin2\omega \end{aligned} \tag{3.23}$$

By writing out the equation above in dq coordinates, one can find the

power coefficients. These are expressed by the matrix equation below.

$$\begin{bmatrix} P \\ P_{cos2\omega} \\ P_{sin2\omega} \\ Q \\ Q_{cos2\omega} \\ Q_{sin2\omega} \end{bmatrix} = \frac{3}{2} \begin{bmatrix} v_d^+ & v_q^+ & v_d^- & v_q^- \\ v_d^- & v_q^- & v_d^+ & v_q^+ \\ v_q^- & -v_d^- & -v_q^+ & v_d^+ \\ v_q^+ & -v_d^+ & v_q^- & v_d^- \\ v_q^- & -v_d^- & v_q^+ & -v_d^+ \\ -v_d^- & -v_q^- & v_d^+ & v_q^+ \end{bmatrix} \begin{bmatrix} i_d^+ \\ i_q^+ \\ i_d^- \\ i_q^- \end{bmatrix} \tag{3.24}$$

What is desireable is to make the active power oscillations equal to zero. By setting $P_{sin2\omega}$ and $P_{cos2\omega}$ equal to zero one aquires the following equation:

$$\begin{bmatrix} 0 \\ 0 \end{bmatrix} = \begin{bmatrix} v_{x,q}^- & -v_{x,d}^- & -v_{x,q}^+ & v_{x,d}^+ \\ v_{x,d}^- & v_{x,q}^- & v_{x,d}^+ v_{x,q}^+ & \end{bmatrix} \begin{bmatrix} i_d^+ \\ i_q^+ \\ i_d^- \\ i_q^- \end{bmatrix} \tag{3.25}$$

By solving for i_d and i_q, one would have the required references in order for these terms to be zero. This results in:

$$\begin{bmatrix} i_d^{-*} \\ i_q^- * \end{bmatrix} = - \begin{bmatrix} v_{x,d}^+ & v_{x,q}^+ \\ -v_{x,q}^+ & v_{x,d}^+ \end{bmatrix}^{-1} \begin{bmatrix} v_{x,d}^- & v_{x,q}^- \\ v_{x,q}^- & -v_{x,d}^- \end{bmatrix} \begin{bmatrix} i_d^+ \\ i_q^+ \end{bmatrix} \tag{3.26}$$

This should in theory then limit the power oscillations. This is, however, not as straigh forward as one might assume. Because even though one can use this method to eliminate the power oscillations, there will still be oscillations in reactive power, as the negative sequence voltages will be non-zero, and there will flow positive sequence current through the system.

[12] and [13] describes how one can choose to control negative sequence current to obtain either constant power or reactive power, balanced grid currents, limited unbalance factor or average power delivery with limited oscillating power. The key to obtain these results, is to let the in phase components of the power coefficients computed above cancel each other out. The articles gives a method to compute different referencs that can achieve this. This thesis's method is slightly adapted, as the method in the article requires the active and power required to be transmitted to be known in advance. Since this is not very practical when transmitting power from an uncontrollable source such as wind, the current references are altered, but the filosophy remains the same. In the equations stated above, the NSC references are chosen to make the terms in the $P_{sin2\omega}$ and $P_{cos2\omega}$ to dissapear. The same procedure can be used to achieve zero reactive power oscillations. The method used is similar to the method described in [12] refered to as

"Positive-Negative-Sequence Control", whereas making reactive power oscillations equal to zero would be the equivalent to "Average Active Reactive Control". The interesting part about this is that the article also describes how these two methods can be combined in order to partially control active and partially control reactive power. Then a trade off can be made concerning:

- How large active power oscillations one will allow, which will result in oscillations in the DC link.
- How large reactive power oscillations one will allow, which will affect operating losses and the magnitude of the current running in the system.
- How important is the current waveform in the system
- How important is it to transfer the maximum available amount of power from the DC link.

It is suggested for a topic of further work that it is found a way to partially control both active and reactive power in order to optimize the controller when active power transfer is an unavialable parameter for the NSC reference generation, so that a more flexible control system can be made.

3.5 Negative Sequence Current Controller

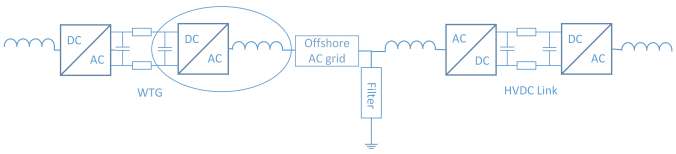

Figure 17: Locations Relevant for NSCC

If one consideres the possibility to use the current references obtained in the previous section to control the system, one would need to construct an additional controller and separate the positive and negative sequence current. The process of seperating the sequences can be done with a Second Order Generalized Integrator Quadrature Signal Generator (SOGI QSG). The positive sequence network would be identical to the standard controller, while the negative sequence network would have a reference generation according to the previous section. For the negative sequence part of the controller, one would no longer use ω as speed and θ as angle, but rather $-\omega$ and $-\theta$, as the SRF is rotating in the opposite direction compared to the positive sequence SRF. The ICC in the negative sequence controller would therefore have opposite signs in the ωL feedforward loops. The control vision can be envisioned in figure 18

The notch filters on the DC link current and DC voltage is there in order to remove 100 Hz oscillations that arises during unbalanced conditions. If these oscillations are not removed, it will in practise mean that the PSCC will be controlling both positive and negative sequence current, which means there are two controllers with the same control objective. This may lead to instability.

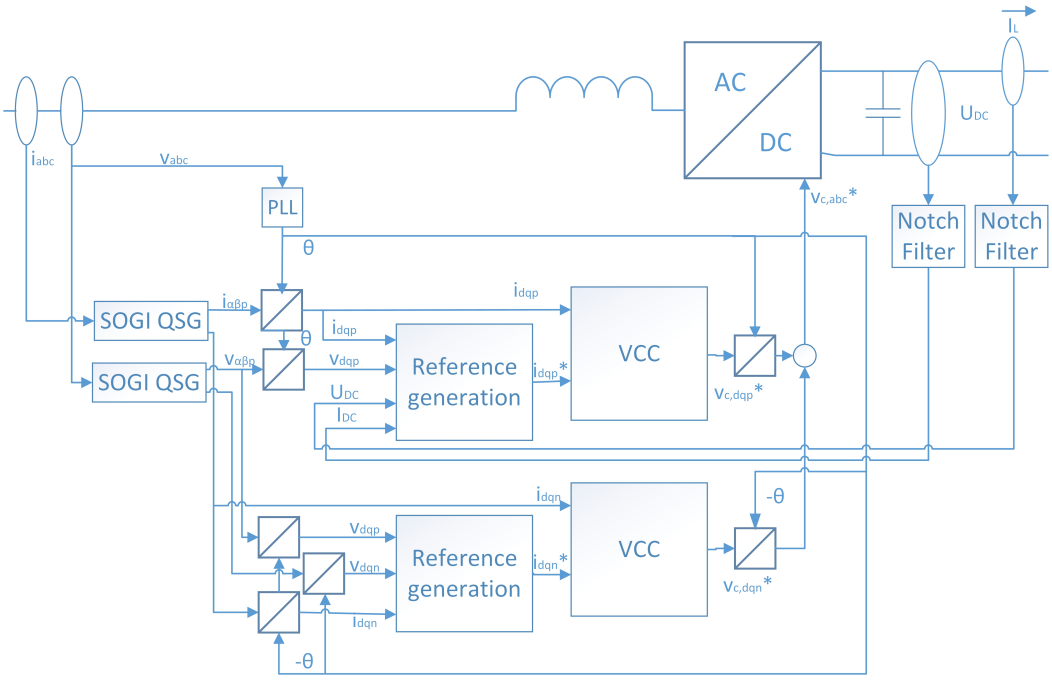

Figure 18: The Control Scheme applied in the model with PSCC and NSCC

4 System Overview

This section will present the model with the specific components created in Matlab SIMULINK, along with the various control systems of the model. The various controllers are presented, and have been simulated with references set as step functions in order to confirm that they are working correctly. A simulation run of the system is performed to confirm that the total system is stable, and to study what is happening during the start-up period, stabilization period, fault event and second stabilization period.

4.1 The modeled system

This section will describe the modeled offshore wind farm, modeled in Matlab R2011b SIMULINK with SIMPOWER systems. Network components will be presented, then the control elements and control systems, before the entire model is presented with general control objectives. Data is mainly taken from [6].

4.1.1 System Layout

The WPP layout is depicted in figure **??**. This show an aggregated turbine with the installed power of 1 GW, and a rated voltage of 4 kV line to line rms. The aggregated WTG is equipped with a b2b converter where the DC link voltage is 8 kV from pole to pole.

The wind turbine transformer steps up the voltage from 4 kV to the park level of 36 kV, before the plant step-up transformer sets the HVDC link voltage at 132 kV. The HVDC link has a rated voltage of 300 kV from pole to pole, and the onshore grid has a rated voltage of 132 kV. In reality, the voltage ratings of the WPP would be higher due to the very high power rating. The onshore grid would have a higher rating, probably 300 kV or higher. This in turn would lead to a need for higher DC link rating, which would be 500 kV or higher. This would mean that plant step up transformer would have a higher rating, that would be close to the rated value of the onshore grid. Further studies should evaluate a more realistic scenario for the onshore grid connection and WPP ratings, especially if GCR should be tested.

In parallel with the aggregated WTG is the NOWITECH turbine, with the same voltage levels and architecture as the aggregated WTG. The turbine employs a full switch model, while the aggregated turbine uses an average switch model at the turbine side. This is due to that the turbine side voltage does not have a significant impact on the transient phenomena studied in

this thesis. However, it is interesting to compare the difference between the average model voltage waveforms and the switched model voltage waveforms. Should the turbine itself be accurately studied in further studies, the full swich model is the preferred model for a more accurate result.

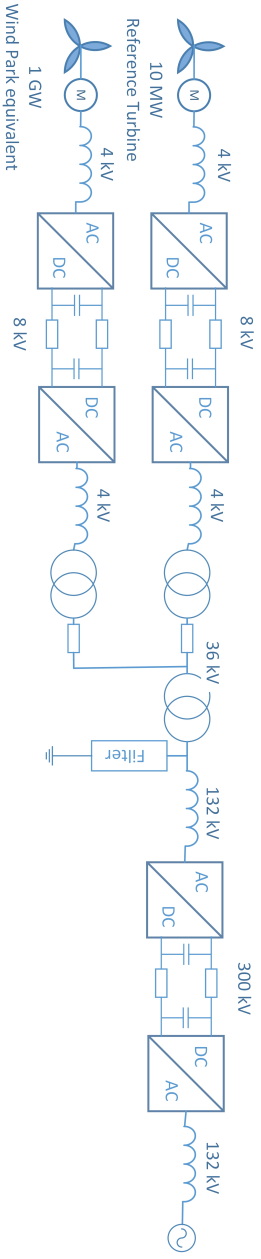

Figure 19: System Layout

4.1.2 Aggregated Wind Turbine Generator

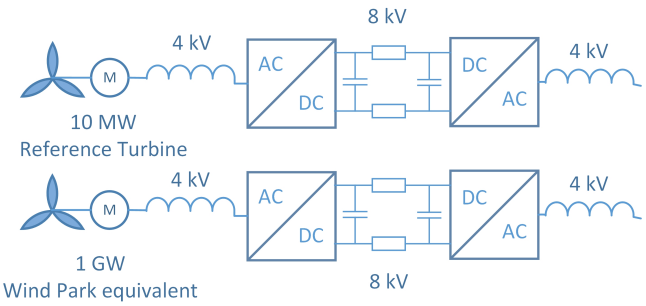

Figure 20: Aggregated WTG and NOWITECH Reference Turbine

The wind farm turbines are all equipped with only permanent magnet synchronous generators (PMSG), with full scale converters that employee VSC technology. This type of turbine configuration is becoming more and more popular due to good characterstics such as wide range of variable speed operation [14]. The mechanical gear can be eliminated by employing many pole pairs and low speed operation, resulting in a Direct Drive solution. This provides a higher degree of reliability, as gear boxes has a bad track record [15]. The wind turbine generator is modelled as a synchronous machine with constant internal voltage and not a PMSG due to easier Matlab modelling. This will not give a significant change of the results, as generator dynamics are not very relevant due to quite stable network conditions at the stator terminals. Generator parameters are listed in Appendix A.

Since this project is only looking at fault events with very short duration, it is acceptable to model the aggregated WTG as operating under constant wind conditions.

The voltage levels for the generator and the back to back (b2b) converter is determined from data provided by the NOWITECH group [5]. The b2b voltage is different in the simulation model compared to the value defined in the reference turbine data, which is 6.5 kV. The reason for this discrepancy is that a rated pole to pole DC voltage of 6.5 kV results in a modulation signal slightly higher than 1, leading the converter voltage to become overmodulated very easily.

$$m_a = \frac{2\sqrt{2}v_{l,l}}{\sqrt{3}U_{DC}} = \frac{2\sqrt{2}\ 4kV}{\sqrt{3}\ 6.5kV} = 1.005 \tag{4.1}$$

This is troublesome during transient network conditions, so the DC volt-

age have been increased in order to have better margins, and it is suggested that the reference turbine specification is updated to 8 kV. This opens up for more focus on the NSCC and PSCC rather than focusing on to have a correct modulation index.

The data for the WTG is:

$$\begin{aligned} &P_n = 1000MW \\ &U_{DC,poletopole} = 8kV \\ &I_{DC} = 125kA \\ &f_{switch} = 1500Hz \\ &C_{DC} = 2\frac{P_{DC}\tau}{U_{DC}^2} = 2\frac{1000MW10^{-2}s}{8kV^2} = 313mF \end{aligned} \tag{4.2}$$

The NOWITECH reference turbine has identical specs to the aggregated WTG, with the exception of the power rating, DC current and capacitor values, which are:

$$\begin{aligned} &P_n = 10MW \\ &I_{DC} = 1.25kA \\ &C_{DC} = 2\frac{P_{DC}\tau}{U_{DC}^2} = 2\frac{10MW10^{-2}s}{8kV^2} = 3.13mF \end{aligned} \tag{4.3}$$

Since the system is built up of two capacitors, one for each pole, each capacitor will have double rating of the numbers stated above due to a series connection of the two capacitors as seen from the plus pole to the minus pole. The system also uses reactors, whose vaules have been set to:

$$\begin{aligned} &L_{WTG} = 0.2L_{n,WTG} = 10.186\mu H \\ &L_{RT} = 0.2L_{n,RT} = 1.0186mH \end{aligned} \tag{4.4}$$

The converter have been modelled with 6 individual IGBTs with diodes, found as a standard SIMPOWER systems block in SIMULINK. The converter set-up is shown in figure 21. The converter uses IGBTs with snubbers, where:

$$\begin{aligned} &R_{on} = 10^{-6} \\ &R_s = 100k\Omega \\ &C_s = Infinite \end{aligned} \tag{4.5}$$

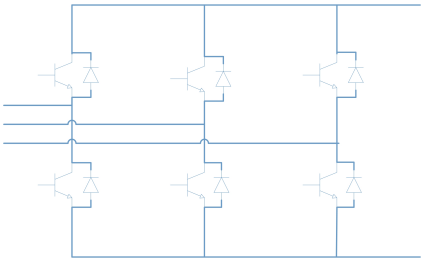

Figure 21: Converter

4.1.3 Offshore AC Grid

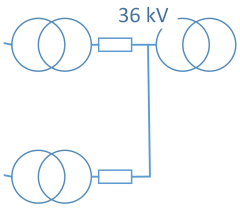

Figure 22: Offshore AC Grid

The voltage ratio of the WTG transformer is 690V/36kV. Connection is yD and leakage reactance is assumed to be 0.05. No load losses and copper losses are assumed to be 0.01 pu. The base power of the transformer is 1000 MW

The system is rated for 900 MW with a power factor of 0.9, giving S_n = 1000 MVA. Rated voltage for the HV cables between the converter transformer and converter is 132 kV, giving a rated current of 4.37 kA. From ABB's XLPE submarine cable data sheet [17], the data for four 132 kV $1000mm^2$ cables can be found from Table 47, with 0.5 km of cables between the converter transformer and the converter:

$$\begin{aligned} R &= \rho l/A = 2.1\mu\Omega \\ C &= 0.5\mu F \\ L &= 44\mu H \end{aligned} \tag{4.6}$$

The rating for the park cable is 36 kV, which results in a rated current of 16.04 kA. The data for 20 of 36 kV $1000mm^2$ cables gives from Table 47, with an average distance of 3 km of cables between the converter transformer and the converter:

$$
\begin{aligned}
R &= \rho l/A = 2.52\mu\Omega \\
C &= 8.4\mu F \\
L &= 50\mu H
\end{aligned} \tag{4.7}
$$

The park cable going to the NOWITECH turbine have been computed identically to rest of the farm, only that it is scaled with the power ratio between 1 GW and 10 MW.

The voltage ratio of the main transformer is 36kV/132kV. $S_n = 1000$ MVA, leakage reactance is assumed to be 0.15. No load losses and copper losses are assumed to be 0.005 pu. The transformer is grounded on the LV side with a grounding impedance of 0.00025 pu.

4.1.4 HVDC Link

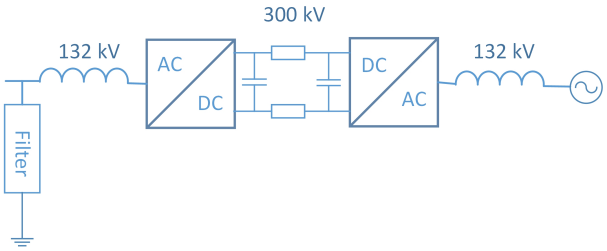

Figure 23: HVDC Link

The data for the HVDC Link is:

$$
\begin{aligned}
P_n &= 900MW \\
U_{DC,poletopole} &= 300kV \\
I_{DC} &= 3kA \\
f_{switch} &= 1950Hz \\
C_{DC} &= 2\frac{P_{DC}\tau}{U_{DC}^2} = 2\frac{900MW10^{-2}s}{300kV^2} = 400\mu F
\end{aligned} \tag{4.8}
$$

$$
L_{Link} = 0.15L_{n,Link} = 8.3mH \tag{4.9}
$$

The snubber design and converter set-up is identical to the WTG converter.

The filter used is a 39^{th} harmonic filter, which has a reconance frequency ω_r of 1950 Hz, VAr compensation of 0.06 pu and a quality factor Q of 25.

$$\begin{aligned} VAr &= 60MVAr \\ C &= \frac{VAr}{\omega_r V_n^2} = 0.28\mu F \\ R &= \frac{Q}{\omega_r C} = 17.424k\Omega \\ L &= \frac{1}{\omega_r^2 C} = 23.7mH \end{aligned} \tag{4.10}$$

With a voltage of +/- 150 kV, and a power rating of 900 MW the current in the DC cables to shore become 3 kA. With an assumed current densitiy of $1.2A/mm^2$, this gives a required cable section area of $2500mm^2$. A cable with a cross section of $2500mm^2$ have been chosen. Distance to shore is assumed to be 100 km, resulting in the cable data:

$$\begin{aligned} &Currentdensity = 1.2A/mm^2 \\ &Crosssection = 3000/1.2 = 2500mm^2 \\ &r_{cable} = 28.21mm \\ &\rho_{cu} = 1.68 * 10^{-8}\Omega/m \\ &l = 100km \\ &R_{cable} = \rho l/A = 0.67\Omega \\ &L_{cable} = 0.2ln\frac{GMD}{GMR} = 0.2ln\frac{0.15}{e^{-\frac{1}{4}} * r} \\ &= 0.384mH/km = 38.4mH \\ &C_{cable} = \frac{2\pi\epsilon_0\epsilon_r}{ln\frac{GMR}{GMD}}10^9 = 0.107\mu F/km = 10.7\mu F \end{aligned} \tag{4.11}$$

Where GMD is the geometrical mean distance between the two conductors and the GMR is the geometric mean radius. [16]

4.1.5 Control System Blocks

The PLL retrieves the angle from the q-axis voltage component, as shown in figure 24 [18]:

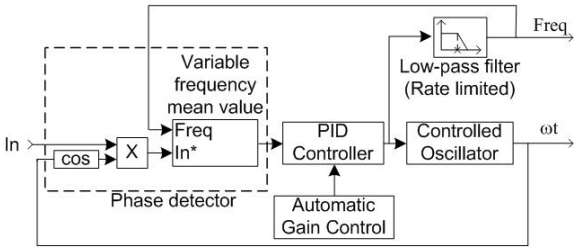

Figure 24: PLL block

The PLL block is used in the onshore converter, the generator side WTG converter and on the PS WTG converter. The SIMULINK 3 Phase PLL block syncs the d axis -90°lagging compared to standard practise where the d axis is synced to the phase a line to neutral voltage. Since all Park Transformation and Inverse Park Transformion blocks in SIMULINK are adapted to this philosophy, the onshore converter and the WTG generator side converter uses this block without any adaptions. However, in the PS WTG converter, all transformation blocks are built from scratch in order to have full control over $\alpha\beta$ and dq variables both in the positive SRF and the negative SRF. The park transform used in this thesis is given so that the d axis voltage must be aligned with the phase a line to neutral voltage. The angle θ output from the 3 Phase PLL block in the WTG PS converter is therefore shifted 90°before it is used to generate the $sin\theta$ and $cos\theta$ signals required for the park transformation.

Furthermore, the PLL requires $v_{abc,n}$ voltage as an input. However, all voltage measuments in the SIMULINK model is done with line to line values due to the fact that line to neutral voltages often are difficult to measure in this type of system. To compensate the phase shift for this type of measurment, the following block is used to generate $v_{abc,n}$ per unit values from the measured line to line voltages [7]:

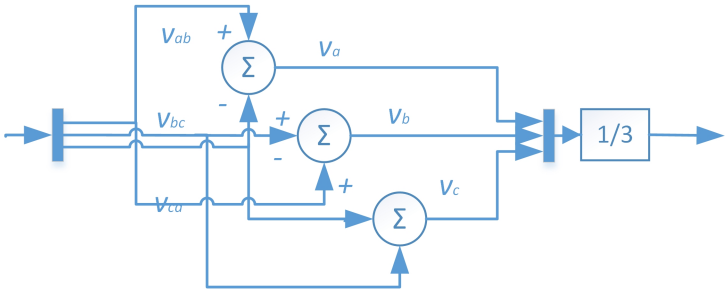

Figure 25: Phase Adjustment Block

The Second Order General Integrator Quadrature Signal Generator is shown in figure 26. The SOGI-QSG extracts the positive and negative sequence components from the $\alpha\beta$ input.

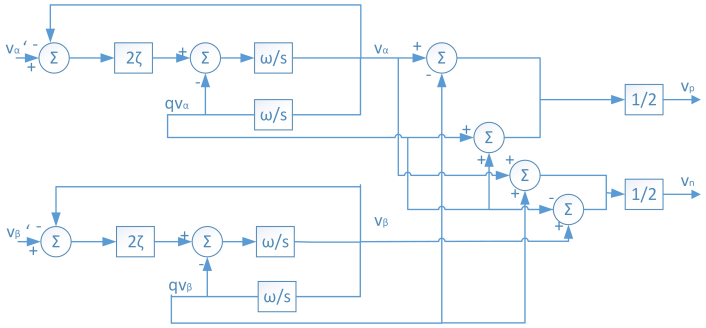

Figure 26: SOGI QSG

The constant k is chosen to be $\sqrt{2}$ to achieve critical damping in the voltage SOGI. For the current SOGI, the most suitable k is found experimentally to be $2\sqrt{2}$.

The notch filter in this thesis are made with SIMULINK transfer function blocks according to [19]. This gives the following transfer funciton for a notch filter:

$$\frac{s^2 + \omega_n^2}{s^2 + \frac{Q}{w_n}s + \omega_n^2} \tag{4.12}$$

Where ω_n is equal to 100 Hz, and Q has been found experimentally to be 200. A filter that removes the 100 Hz oscillations can also be made by using a SOGI tuned to 100 Hz, in stead of 50 Hz. One can subtract the input signal with the filtered signal from the SOGI, since this will be the 100 Hz component in the input signal.

4.2 The Simulation Model's Control System

4.2.1 Inner Current Control Loop

The control parameters of the inner current control loop in the WTG converters and the HVDC link converters have been tuned to the values presented below. For more information tuning of the controller parameters of the controller system, consult Appendix D:

$$\begin{aligned} K_{p,HVDC} &= 0.93 \\ K_{i,HVDC} &= 15.99 \end{aligned} \tag{4.13}$$

$$\begin{aligned} K_{p,WTG} &= 0.57 \\ K_{i,WTG} &= 6.92 \end{aligned} \tag{4.14}$$

The angle reference used for the park transformation is set stiff in the PS HVDC link converter, and is found by using a PLL in the other converters. Thus the PS HVDC link converter is the master and the WTG PS converter is the slave in the offshore AC grid in this setup. Poor tuning of the PS HVDC link converter then becomes very problematic, as the voltage waveforms might become so distorted that the PLL in the PS WTG converter has problems syncing to the system creating an unstable system.

This thesis have exclusively been using VCC. [20] used a PR controller for the WTG converter in order to be able to control the frequency in the AC collector grid, while in this thesis, frequecy is controlled by a stiff reference in the PS HVDC link converter. This means that the WTG converter must use a PLL to synchronize the controller to the AC grid, which can prove challenging during transients such as start-up sequences and faults. A PR controller might give a more flexible adjustment of AC frequency, making it a more robust solution for the offshore grid during faults. It also has the ability to inject any harmonic components into the grid by placing several PR controllers in parallel, making the AC voltage wave form smoother and more distorion free. Most importantly, it removes the needs for park transformations, and therefore also PLL blocks. It does have the negative advantage that it is unable to regulate negative sequence current injection to stablize DC voltage for network conditions where the amount of negative sequence voltage almost equals the positive sequence voltage. This is due to the mathemtical formulation of the current references in the NSCCs when a PR controller is used. A topic for further research might be to use the two models for the PR and the VCC controllers to compare their ability to effectively regulate the offshore AC grid during faults.

4.2.2 Grid Side HVDC Link Converter

The control objectives of this converter controller is to keep the HVDC link DC voltage constant, and to control the amount of reactive power which enters the onshore grid. GCR often dictates an amount of reactive power the WPP should be able to deliver and absorb. During faults close to the converter in the onshore grid, the voltage will drop, limiting the converter's ability to control the DC link voltage. In these instances, the role of keeping the DC voltage constant might be transfered to the offshore grid converter. Detecting a fault in the onshore grid and communicating the change of control strategy to the offshore converter can be done with different methods [21]. This thesis will not consider these kinds of faults, and the onshore converter will therefore at all times control the DC link voltage. It is however recommended to implement such a control system if research regarding short circuits in the onshore grid will be conducted.

The control parameters of the outer control loop have been tuned to the following values according to the methods presented in Appendix D:

$$\begin{aligned} K_{p,DC} &= 10.56 \\ K_{i,DC} &= 21.22 \end{aligned} \tag{4.15}$$

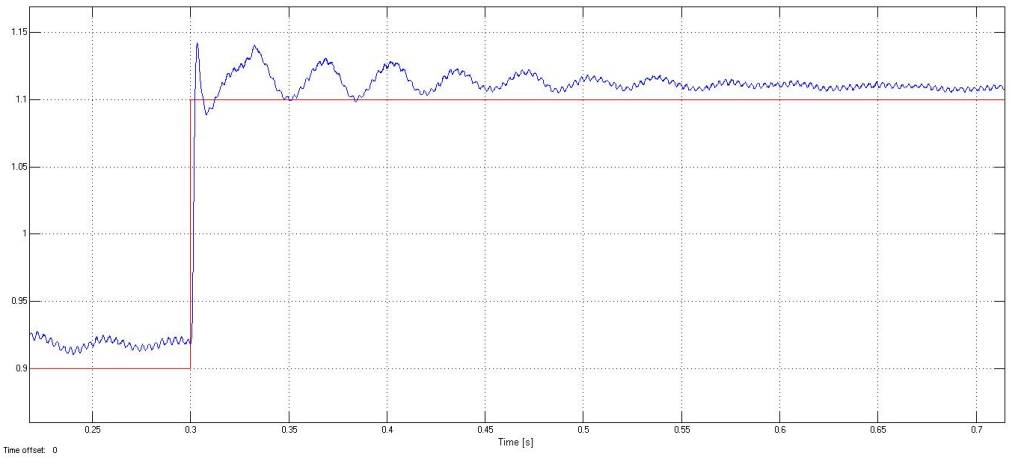

Figure 27: DC Voltage Step Response in the GS HVDC Link Controller

$$\begin{aligned} K_{p,Q} &= 6.25 \\ K_{i,Q} &= 12.57 \end{aligned} \tag{4.16}$$

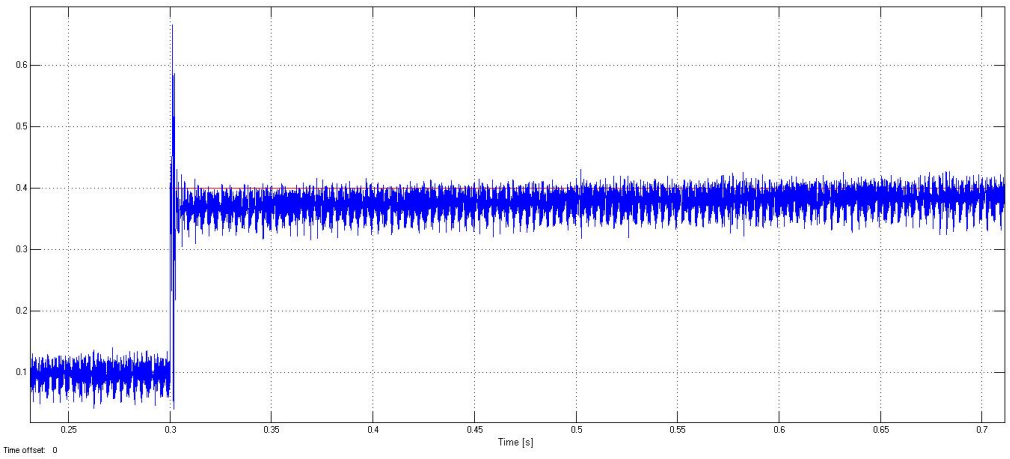

Figure 28: Reactive Power Step response in the GS HVDC Link Controller

Figure 27 shows that the controller step response is slightly oscillatory. However, it is desireable to keep the proportional gain high in order to have a quick response from the controller. For the same reason, the step response shown in 28 is accepted even though there is a quite large overshoot in the reactive power through the converter.

4.2.3 Offshore HVDC Link Converter

The control objectives of this converter controller is to keep the voltage in the offshore AC grid constant. This converter also sets the frequency in the offshore AC grid by connecting a stiff three phase signal to the PLL block that sets up the angle used in the park transformation. This converter can also be used to inject negative sequence current into the offshore AC grid, however the model in this thesis does not take advantage of this posibility. For the reasons mentioned in the previous subsection, this converter will always be used to control the AC voltage in the offshore wind farm in the simulations considered in this thesis.

The control parameters of the outer control loop have been tuned to the following values according to the methods presented in Appendix D:

$$\begin{aligned} K_{p,AC} &= 0.75 \\ K_{i,AC} &= 1.5 \end{aligned} \tag{4.17}$$

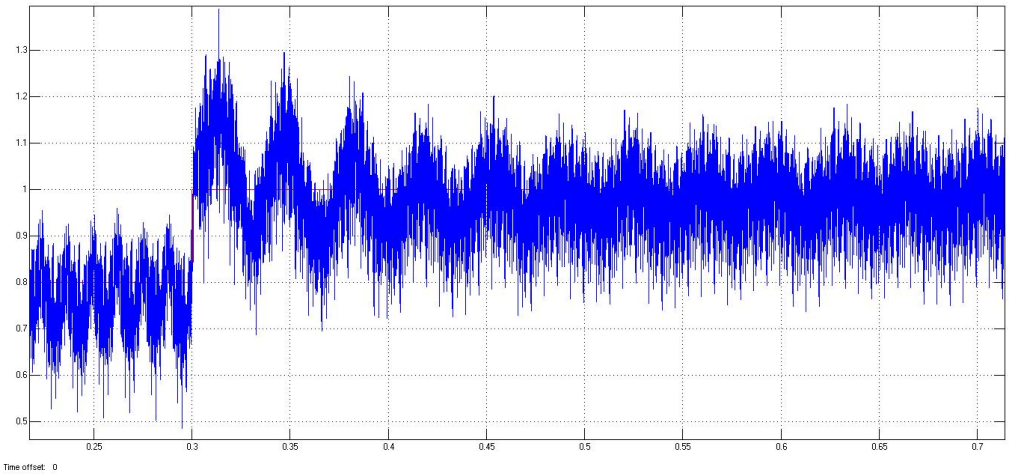

Figure 29: D axis AC Voltage Step Response in the PS HVDC Link Controller

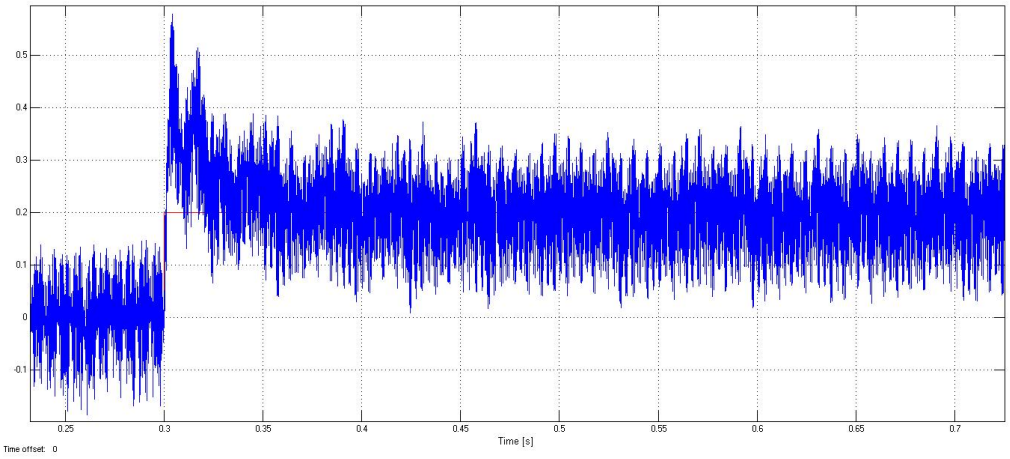

Figure 30: Q axis AC Voltage Step Response in the PS HVDC Link Controller

The two figure 29 and 30 show a similar characterstic to the two characteristics in the onshore HVDC link converter. Here the i_d outer loop controller shows a slightly oscillatory response, while the i_q outer loop controller has medium a medium sized overshoot. Since much of the dynamics in the converters are similar for the two HVDC link converters, it is not surprising that these two responses are similar to the onshore HVDC link converter responses.

4.2.4 Park Side WTG Converter

The control objectives of this converter controller is to keep the DC voltage in the b2b converter constant and to control the amount of reactive power delivered into or absorbed from the offshore AC grid. This converter is also used to inject NSC into the offshore AC grid to prevent oscillations in the DC voltage during unbalanced faults.

The control parameters of the outer control loop have been tuned to the following values according to the methods presented in Appendix D:

$$\begin{aligned} K_{p,DC} &= 1.18 \\ K_{i,DC} &= 2.38 \end{aligned} \tag{4.18}$$

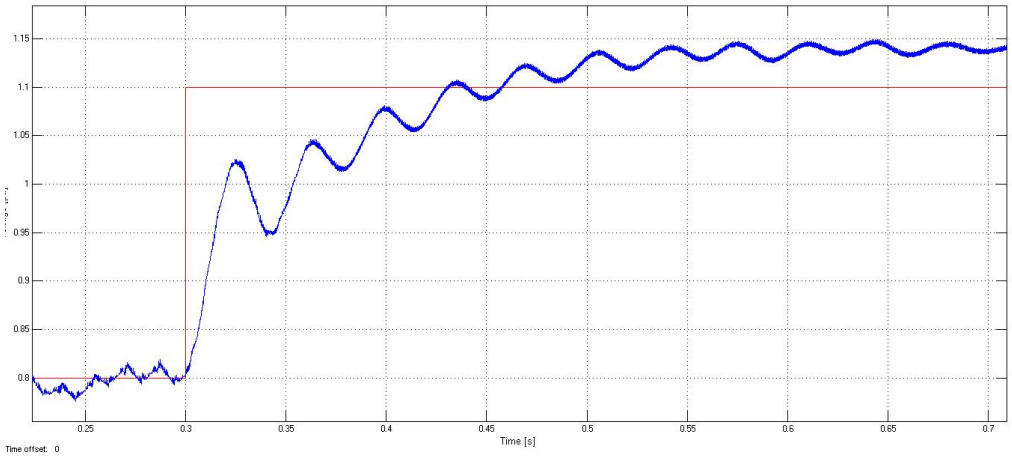

Figure 31: DC Voltage Step Response in the PS WTG Controller

Figure 31 shows that the voltage controller is slow and slightly oscillatory, with a seemingly large steady state deviation. This large deviation is closed in by the integral effect of the controller over time, but due to the time constant of the inner current loop, the integral part of the controller cannot have a stronger effect, making the controller slow to react to changes in the reference signal. The reason for the oscillatory behaviour is that the controller's proportional constant is close to the stability limit, even though it is desired that the controller should be faster. The solution to this problem could be to add a derivative effect to the PI controller, and thus to have a PID controller for better stability margins. However, due to the added complexity of this solution, a PID controller has not been implemented, but

it is suggested that this might be an addition to the DC voltage controller in further use of the model.

$$\begin{aligned} K_{p,Q} &= 9.37 \\ K_{i,Q} &= 18.84 \end{aligned} \tag{4.19}$$

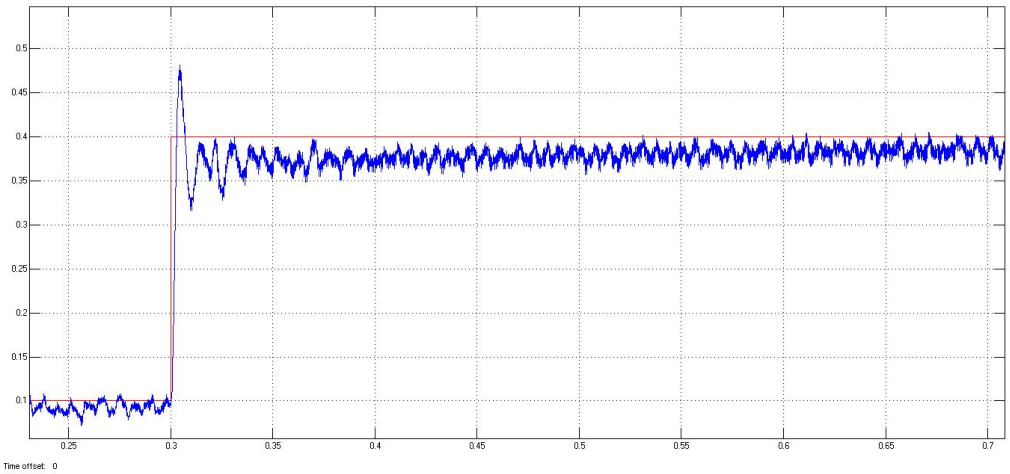

Figure 32: Reactive Power Step Response in the PS WTG Controller

As figure 32 shows, the reactive power controller responds quickly to the change in the reference. The tuning of the Q controller of the WTG converter was crucial to establish stability in the total system, and the stability margins of this controller has experimentally been found to be very small. The reason for this is perhaps due to the fact that with a negative sequence controller the system that is controlled will have more free variables than the controllers degrees of freedom, this is described more in detail in chapter 3.4.1. During NSC injection, oscillatory active power in the system is controlled to be zero, leaving oscillatory reactive power an unregulated system parameter. During steady state balanced conditions, this should be zero by default. However, due to numerical challenges in the start-up phase of the simulations, as well as the effect of the time SOGI blocks need to adjust etc, there will be a component of NSC in the system, even though the system theoretically should be free for negative sequence components. This will mean that unless the controller is quick and stable, the NSCC and the reactive power controller might influence each others negatively, creating a large deviation in both the NSCC, and the reactive power controller.

The NSCC should theoretically be an almost exact copy of the positive sequence VCC. However, expertimental tuning have found that slightly higher value for K_p, and a time constant that is much larger than the time constant used in the positive sequence VCC, should be used in order to achieve stability. Furthermore, the voltage feedforward terms are neglected in this controller, as this gives a very poor response during transient conditions.

$$\begin{aligned} K_{p-} &= 0.57 \\ K_{i-} &= 6.92 \end{aligned} \tag{4.20}$$

4.2.5 Turbine Side WTG Converter

In this master thesis, the study of faults and transients in the electrical network means that the timeframe required for simulations is much smaller than for the mechanical system of the wind turbine. The fault in the AC network is cleared after 120 ms, while the mechanical time constant for the wind turbine is 2.65 seconds. The speed up effect of the wind turbine is thus very small during faults studied in this master thesis, and references from the WTG converter is therefore almost constant during the fault simulations. The turbine also delivers roughly the same amount of power during the fault, as it feeds the DC chopper in the b2b converter, as shown in figure 38

Due to these reasons, limited time have been used to establish a detailed model of the turbine generator itself. When the simulation model is required for further research regarding the NOWITECH reference turbine, it is recommended that the level of detail is raised. The PI controller used to regulate electrical power has been tuned to the values given below. For more information tuning of the controller parameters of the controller system, consult Appendix D:

$$\begin{aligned} K_{p,HVDC} &= 0.93 \\ K_{i,HVDC} &= 15.99 \end{aligned} \tag{4.21}$$

5 Simulation results

This section presents the simulation results from the short circuits on the points A, B and C indicated in figure 33. The fault is applied for 120 ms, before it is cleared. When ground is involved, the resistance to ground is set to 0.05 pu. The effects of Single Line to Ground (SLG), Double Line (DL) and Double Line to Ground (DLG) type of faults have been studied with and without the NSCC, in order to compare the effect of seperately controlling the positive and negative sequence during unbalanced fault conditions. A symmetrical three phase fault is also studied, in order to see whether the two control philosophies performs equally good during balanced conditions, which they in theory should. The goal of controlling the negative sequence controller is to inject NSC to prevent active power oscillations, in order to prevent 100 Hz oscillations on the DC link voltage. The simulation results are therefore presented as DC voltage in the HVDC link and b2b converter. Network voltage at the HVDC link PS converter is also studied, in order to see whether the NSCC has a positive effect on the network voltage. NSC references and the NSC are also studied, in order to see how the controller reacts to the unstable network conditions.

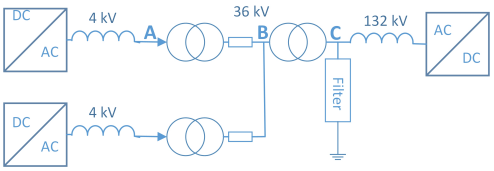

Figure 33: Short Circuit Locations

During the simulations, a discrete time frame was used, and the Matlab solver was set to ode3, Bogacki-Shampine, with a fixed timestep of 3e-6 s. The SIMPOWER systems solver was set to discrete as well, with a fixed timestep equal to the Matlab solver, and solver method was set to Backward Euler. The simulation results are not completely steady state before the fault is applied, the reason for this is the high integral time constant in some of the outer control loops PI controllers. The time required for the system to stabilize completely is quite long, so a compromise has been made between simulation time and closeness to the steady state condition.

During the simulations when a fault is applied at point A and B, the NOWITECH turbine is left out to shorten simulation time. When a fault is applied at point C, the NSCC in the aggregated WTG is disabled. The reason for this is that the NSCC has a negative influence on system stability,

as discussed in 6.1, and so it is more interesting to study the effect of the reference turbine's control system on a stable system than an slightly unstable one. The HVDC link DC voltage, park rms voltage, WTG DC voltage and negative sequence currents has been measured for several scenarios, a total overview over the results can be found in Appendix E. Below, the DLG fault applied at point B and C is studied in figure 34 - 47. The reason for chosing the DLG fault, is that this is the type of fault which generally had the worst effect on the HVDC link DC voltage during the simulations. This figure shows the oscillations in the HVDC voltage during faults, when the NSCC is enabled or disabled. Faults at point A has a so small effect on the HVDC link converter that the results from these measurements are left out.

The next subsection presents a simulation run from start up, until a fault occurs and then until the system has reached a steady state again. Then the fault effects are researcehed in more detail over the next four subchapters.

5.1 The Simulation Run

Starting up simulations in SIMULINK for this type of models can prove challenging. There are integrators that must have a sensible starting value; some places there must be used delay blocks on signals due to the nature of the control system; and in some places the control system must be bypassed the first time steps during simulations to avoid numerical instability. In addition to this, there will be large current oscillations due to quick variations in current magnitude close to inductive elements, and there are capacitive elements in the system that must be charged to achieve stable operating conditions. The starting sequence in this SIMULINK model is therefore not representative for an actual network occurance. The starting sequence in this thesis is done in order to achieve a stable network condition which faults can be tested on, and not in order to depict actual black start operation of a WPP. During an actual black start operation of a WPP, there would be several breaker operations while: charging the DC link; establishing a stable network condition in the AC grid offshore; and sequentially connecting the WTG's.

0.350 seconds into the simulation, a fault occurs. In this particular simulation run, there is a Double Line to Ground (DLG) fault at the low voltage side of the plant step-up transformer. The fault is on for 120 ms before it is cleared, and the simulation run continues until a steady network condition is reached. The wind is blowing at 11 m/s, resulting in power production of about 0.6 pu. All DC voltages are set to 1 pu, and reactive power is set to 0 in the WTG park side converter and the HVDC link onshore converter. The voltage in the offshore wind farm is set to $v_d = 1$ pu and $v_q = 0$ pu.

5.1.1 HVDC Link Onshore Converter

The graphs below depict the simulation run for the onshore converter. The current is seen to rise well above the 1.1 pu limit during start-up, due to the oscillation caused by the reactor, creating a very high DC voltage value that would destroy the converter. This is not a realistic occurance, as the AC grid offshore would not behave like an ideal voltage source, and the converter breaker would be designed in order to limit this current. Power is fed into the DC link from the onshore grid, charging the capacitors in the DC link, and then setting the AC voltage in the offshore wind farm. When this is achieved, the WTG converter starts feeding power into the AC grid, which in turn is fed into the HVDC link, and thus reversing power direction in the onshore converter. When the fault occur, the power direction is reversed so that the onshore grid pumps power into the offshore wind farm. Theoretically, it should be possible to create a HVDC link controller that would sense that the onshore grid was feeding a fault in the offshore wind farm, and then limit the amount of power fed into the wind farm. However, once the NSCC is enabled in the offshore HVDC link converter also, it will need power flow from the onshore grid to inject NSC into the AC offshore grid, so this may or may not be a good solution.

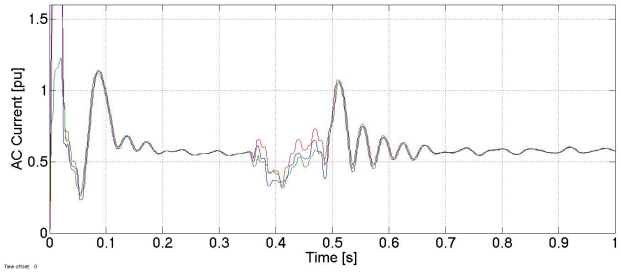

(a) Onshore Grid Current

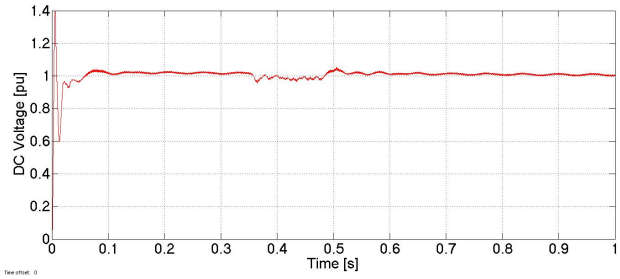

(b) DC Voltage

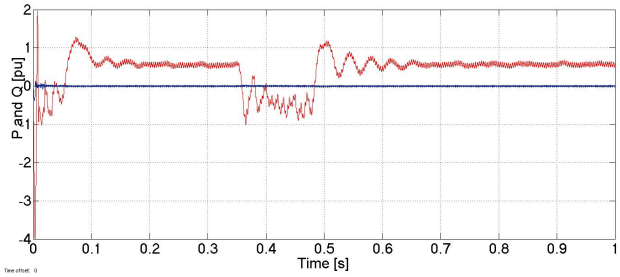

(c) Power and Reactive Power

Figure 34: Simulation Run in the Onshore HVDC Link Converter

5.1.2 HVDC Link Offhore Converter

The graphs below shows the simulation run for the offshore HVDC link converter. The converter sets up the AC voltage in the offshore wind farm, which is not as stable as the onshore grid. The reason for this might be that: this is a weak grid; that there is suboptimal tuning of many controllers, of which some may have competing control objectives, discussed in more detail in section 6.1; or it might be due to voltage quality issues, as discussed below. The slightly unstable network voltage offshore creates a more oscillating DC voltage on the park side of the HVDC link. When the AC voltage approximately reaches it rated voltage, the power flow direction is reversed, and power is fed from the WTG into the HVDC link.

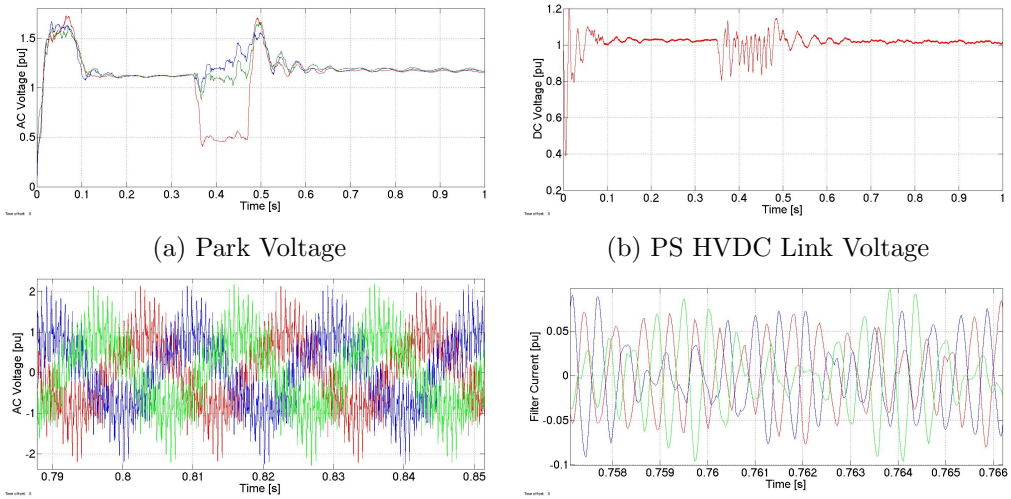

(a) Park Voltage

(b) PS HVDC Link Voltage

(c) Park Voltage Waveform

(d) Filter Current

Figure 35: Simulation Run in the Offshore HVDC Link Converter

In figure 35c the voltage waveform in the AC grid offshore is presented. It is quite distorted. This is in part due to the fact that:

- No harmonic injection is modelled in the WTG converter. In reality, the reference turbine is planned to have 3^{th} harmonic injection [5]
- There is no filter on the WTG converter, normally a LCL filter or another filter would have been implemented here.
- Only a 39^{th} harmonic filter is used on the PS HVDC Link converter, a 78^{th} harmonic filter could also have been used, as well as a general HP filter [6]
- Two level converters are used in this model due to easier implementation of the control system, compared to three level converters or MMCs. These converters would have had smaller harmonic content in the AC voltage.
- In stead of many small WTG's, there is one big, making switching noise from the turbines more defined in the AC collector grid.

None of these soltions are not implemented. This is not done in order to keep the complexity level in the system as low as possible, and because some of the measures mentioned above are beyond the scope of this thesis. It should however be mentioned, that the stability margins of the system in this simulation model could benefit from a more stable and undistorted AC

voltage in the offshore AC grid, and it is recommended that these measures are implemented in part or total during further works with this simulation model.

A picture is also shown of the current into the offshore HVDC link converter filter. Current with 1950 Hz and 1500 Hz frequency can be seen to go through the filter, which is the switching frequency of the HVDC link converter and the WTG converter respectively. A filter at the WTG converter would prevent 1500 Hz oscillations entering the offshore collector grid and flowing into the filter at the PS HVDC Link converter.

5.1.3 WTG Park Side Converter

In the following graphs, the simulation run for the WTG PS converter is depicted. Figure 36a shows the power and reactive power injected into the AC grid from the WTG converter. The power direction is first into the converter, but when the AC voltage in the collector grid is stabilized, the WTG converter starts injecting power, which in turn reverses the power flow in the HVDC link and the rest of the system.

The WTG converter has a DC chopper equipped, which is switched on at voltages above 1.2 pu. Figure 36b shows that the chopper is active during the starting sequence, as the WTG is feeding power from the beginning of the simulation. Then the AC voltage has not yet been stabilized, and the offshore AC grid is thus unable to absorb power from the WTG, leading to excess power in the b2b converter that is dissipated in the DC chopper. Due to the slow integral effect from the DC voltage controller, the DC voltage is not completely stable at 1 pu before a longer timeperiod then what has been modelled. The way that the system has been modelled to start-up, is not realistic. The chopper would not be active in a real scenario, there the wind turbine would stay disconnected until the AC voltage in the offshore wind farm was relatively stable.

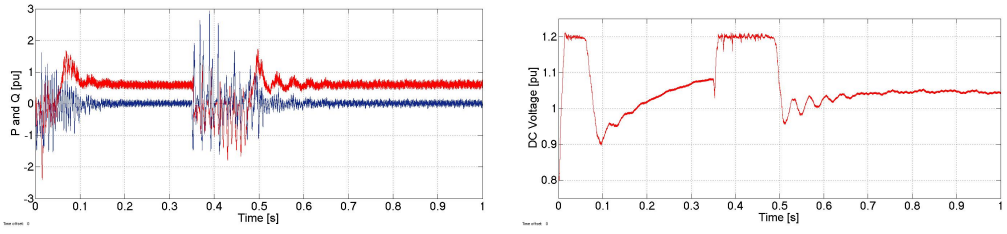

(a) Park Power and Reactive Power (b) b2b DC Voltage

Figure 36: Simulation Run in the Park Side WTG converter

The WTG converter also has a negative sequence controller, where the current references in red, and actual currents in blue, are depicted below for the d and q axis. During balanced network conditions, this controller should have currents and current references equal to zero. However, due to the reasons mentioned in the beginning of this section 5.1, the starting value for both current, and therefore also current references are non-zero. Both current and current references decay to zero after some time, allthough more accurate tuning of the various controllers in the system might make the time before the variables approaches zero value much smaller. Comparing figure 36a and the negative sequence currents, one can see that there is a correlation between power and reactive power oscillations and negative sequence current. This is why finely tuning the Q and U_{dc} controllers is so important, even though the controllers have sequence separation, these two controllers seems to affect one another, and both must be tuned correctly for the system to be stable.

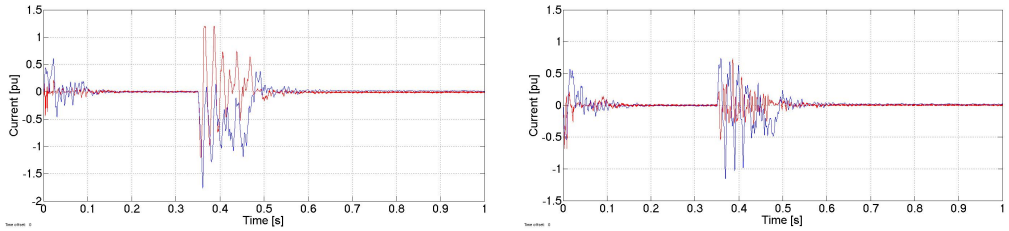

(a) D Axis NSC (b) Q Axis NSC

Figure 37: NSC During the Simulation Run

5.1.4 WTG Generator Side Converter

In this section, both the result from the NOWITECH turbine and the aggregated wind turbine are presented, so that the differences of using a switched model and an average model might be highlighted. It is possible to continue the work done in this section to more accurately study the turbine during different fault scenarios or other events.

The power fed trough the turbine side converter, as well as the turbine speed is shown below.

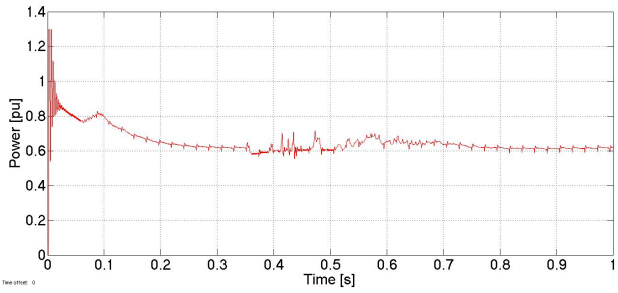

(a) Power from the WTG

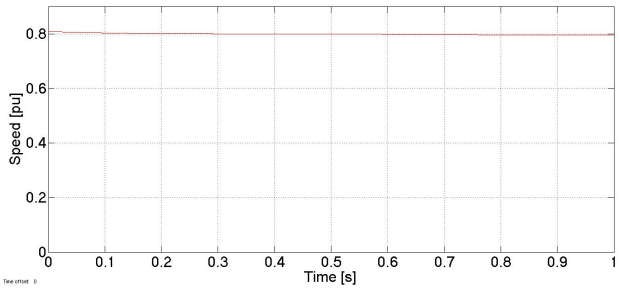

(b) Speed

Figure 38: Rotor Speed and Power from the WTG

The NOWITECH turbine is identical to the aggregated WPP turbine, with the exception of the lower power rating, and the use of IGBTs in stead of an average model at the generator side of the converter. This is done in order to more accurately study the fault effects on the turbine. The differences from the aggregated turbine's and stator voltage for the simulation sequence is presented below.

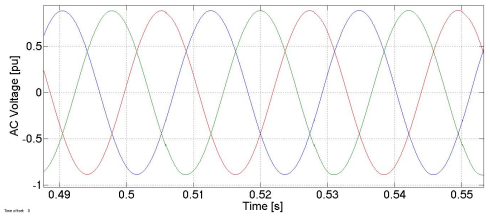

(a) Aggregated WTG

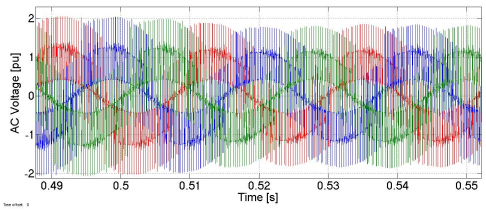

(b) NOWITECH WTG

Figure 39: Comparison of AC Voltage in the NOWITECH and the Aggregated WTG

As one can see, there is quite some difference between the voltage waveforms. The large ripples present are due to the switching action of the IGBTs.

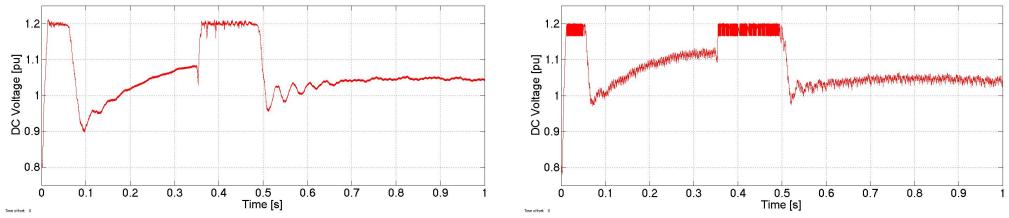

(a) Aggregated WTG (b) NOWITECH WTG

Figure 40: Comparison of DC Voltage in the NOWITECH and the Aggregated WTG

During the fault, the DC voltage in the b2b converter rises due to the decreased capability to inject power into the offshore AC grid. The increased DC voltage causes a slight increase in the stator terminal voltage, but the change is quite small, and the network conditions on the generator side of the WTG converter is almost steady state. The reason to why the DC voltage looks different in the reference turbine, is that when the turbine is included in the simulation model, the NSCC in the aggregated WTG is disabled. Therefore the voltage in the reference turbine does not decrease as much as the voltage in the aggregated WTG during the start-up. The reference turbine should in theory also have more stable waveforms, which it does have, than the aggregated WTG, as this can be seen as an extra turbine connecting to a grid, rather than a turbine that has to stabilize the grid by itself. The reference turbine has more high frequency ripples than the aggregated WTG, which is due to the switched model at the generator side at the b2b converter.

5.2 Fault Effects on the HVDC Link

What can be seen from the graphs below, is that there HVDC link DC voltage oscillations during faults at point B actually are worse when the NSCC is enabled. Oscillations are very high the first cycles, then they are reduced somewhat before an increase again when the fault is cleared at 0.470 s. Examining the reference voltage from the NSCC at figure 49a, one can see the reference signal does not decay to zero when the fault is cleared, but the controller need some time to stabilize. This type of behaviour can be found during other types of faults as well. However, during faults at the converter terminals, point C, it does seem that the NSCC has a positive influence on the DC voltage. This is analyzed in detail in chapter 6.1

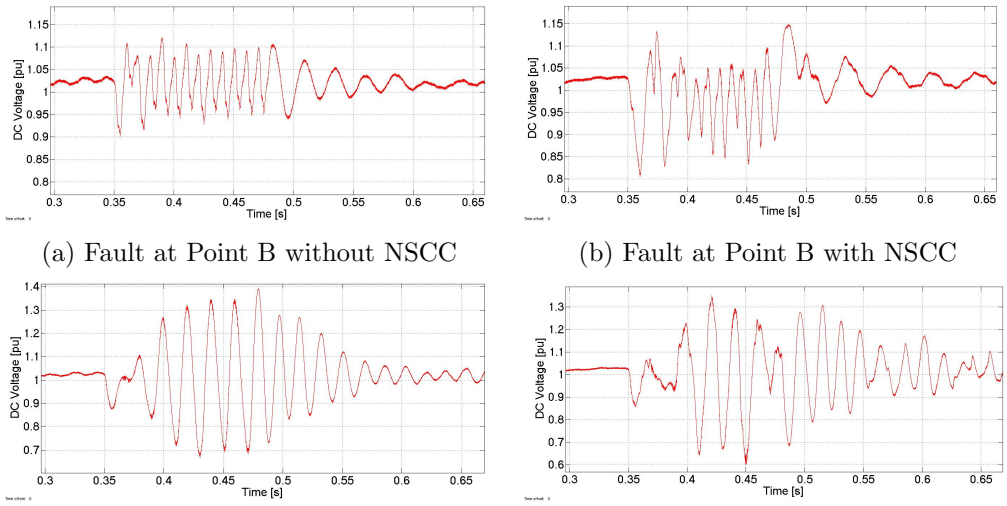

(a) Fault at Point B without NSCC

(b) Fault at Point B with NSCC

(c) Fault at Point C Without NSCC

(d) Fault at Point C With NSCC

Figure 41: HVDC Link Voltage During a DLG fault

Max/Min HVDC Link Voltage		With NSCC		Without NSCC	
Fault Type	**Fault Location**	**Max**	**Min**	**Max**	**Min**
SLG	**C**	1.41	0.72	1.39	0.67
DL	**B**	1.22	0.81	1.125	0.88
	C	1.27	0.79	1.14	0.92
DLG	**B**	1.15	0.82	1.125	0.88
	C	1.35	0.6	1.4	0.7
3PG	**B**	1.3	0.87	1.24	0.87

Figure 42: Summary of HVDC Link DC Voltage During Faults

The table in figure 42 presented above gives a quick overview over maxi-

mum and minimum HVDC link DC voltage during the faults, and the general conclusion seems at the first sight to be that the NSCC significantly worsens the situation in all but one case. However, if one analyze the waveforms for SLG and DL faults at point C presented in the Appendix E in addition to the figure above, one finds that there is a time period some time after the fault has started that there is lower oscillations in the DC voltage than for the case without the NSCC. The reason for this is that, as chapter 6 will present in more detail, the control system is not very well tuned. During transient conditions, it needs some time before it stabilizes. When the control system has had enough time to react to the fault, it improves the oscillations in some of the registered scenarios.

5.3 Fault Effects on the Offshore Grid

During the fault, the voltage v_{ab} drops to zero at the fault location, while the voltage in the healthy phases rises. The situation is not dramatically changed by enabling or disabling the NSCC. In general, voltage in healthy and faulted lines are slightly lower when enabling the NSCC. The reason for this is perhaps that the power flow from the WTG converter is smaller during faults, as part of the power from the wind turbine is used to inject NSC. The voltage peak after the fault is cleared at 0.470 s, is due to the fact that a lot of power is transmitted to the offshore converter before the converter had time to reverse the power flow. This leads to an increase of stored power in the filter capacitor, causing the voltage rise.

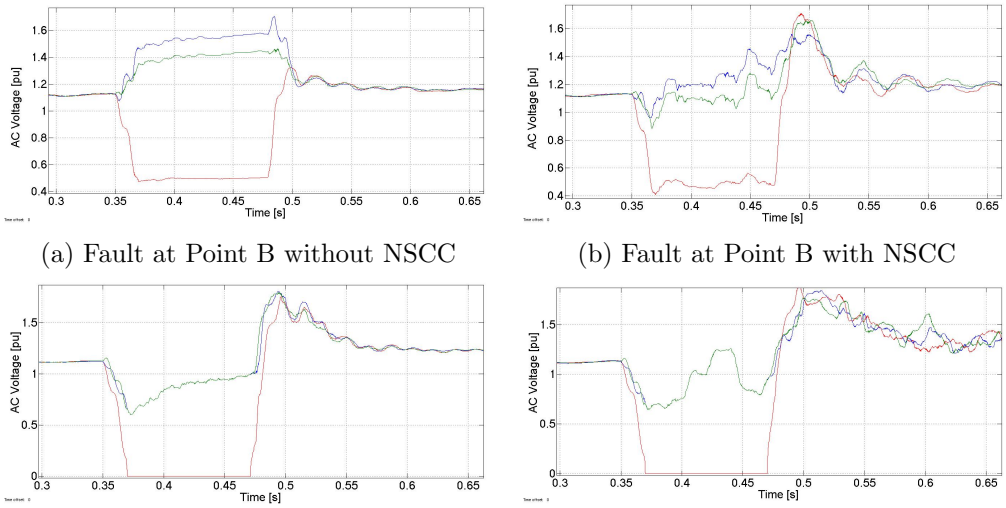

(a) Fault at Point B without NSCC

(b) Fault at Point B with NSCC

(c) Fault at Point C Without NSCC

(d) Fault at Point C With NSCC

Figure 43: Offshore Grid AC Voltage During a DLG fault

5.4 Fault Effects on the WTG PS Converter

Below the b2b DC voltage during the faults scenarios, are presented. The results from a short circuit at point A, next to the reference turbine, is also included. The reason the results from point A is not included in the two previous sections is that the effect on the offshore HVDC link converter of a short circuit near a single turbine is almost negligble in this context.

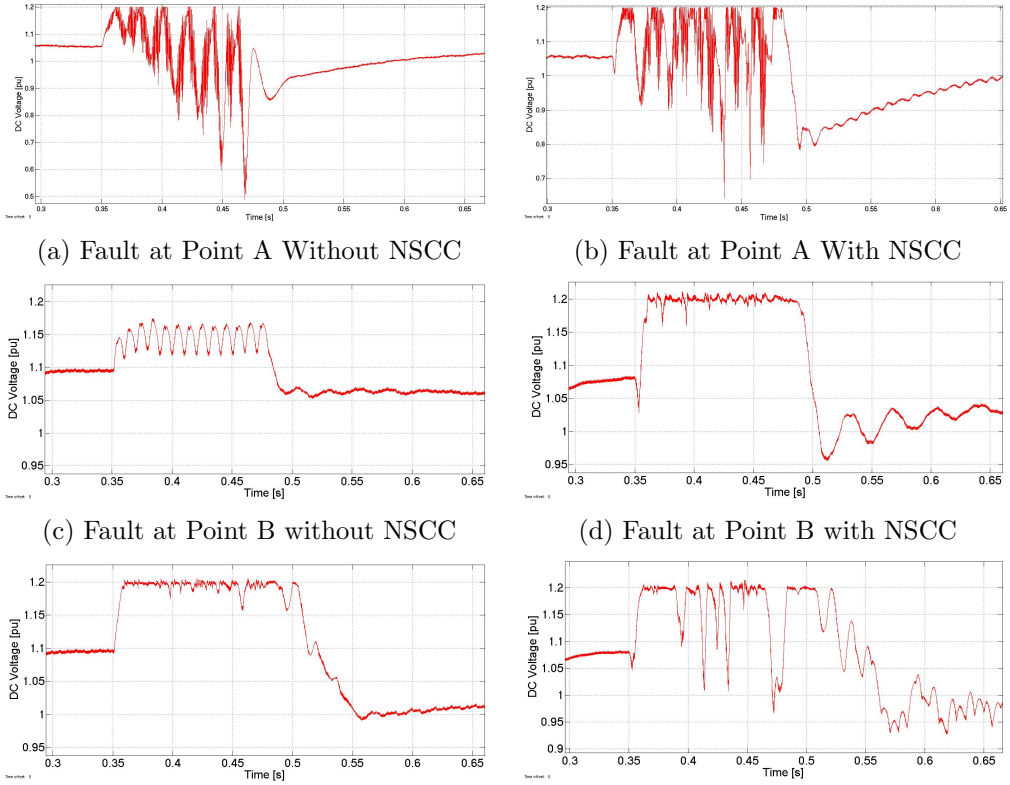

(a) Fault at Point A Without NSCC

(b) Fault at Point A With NSCC

(c) Fault at Point B without NSCC

(d) Fault at Point B with NSCC

(e) Fault at Point C Without NSCC

(f) Fault at Point C With NSCC

Figure 44: WTG DC Voltage During a DLG fault

The results from the WTG DC voltage is very interesting, because it shows that the NSCC creates a worse result than the standard controller in case A and B. The DC voltage rises more quickly when the NSCC is enabled, which means that the chopper eventually is enabled, and power is dissipated rather than transfered to the offshore grid. This is not unexpected, as the converter is unable to deliver the same amount of active power when the capcity to deliver power is also used by the NSCC to inject NSC into the grid. The reason why point C is showing a slightly better outcome than A and B, is that probably there are large oscillations caused by the large NSC

flowing in this case. However, the top point of the DC oscillations are not visible due to the chopper action, only the bottom, which makes it seem like this is an improvement over the standard control system.

As can be expected there is a much larger NSC flowing when the NSCC is enabled, as the two following figures illustrate. This is due to the fact that the goal of the NSCC is to inject current into the grid to counteract oscillations in active and reactive power. The currents are however very large, and the waveforms are non sinusoidal, due to saturations blocks used to limit the current flowing through the converter.

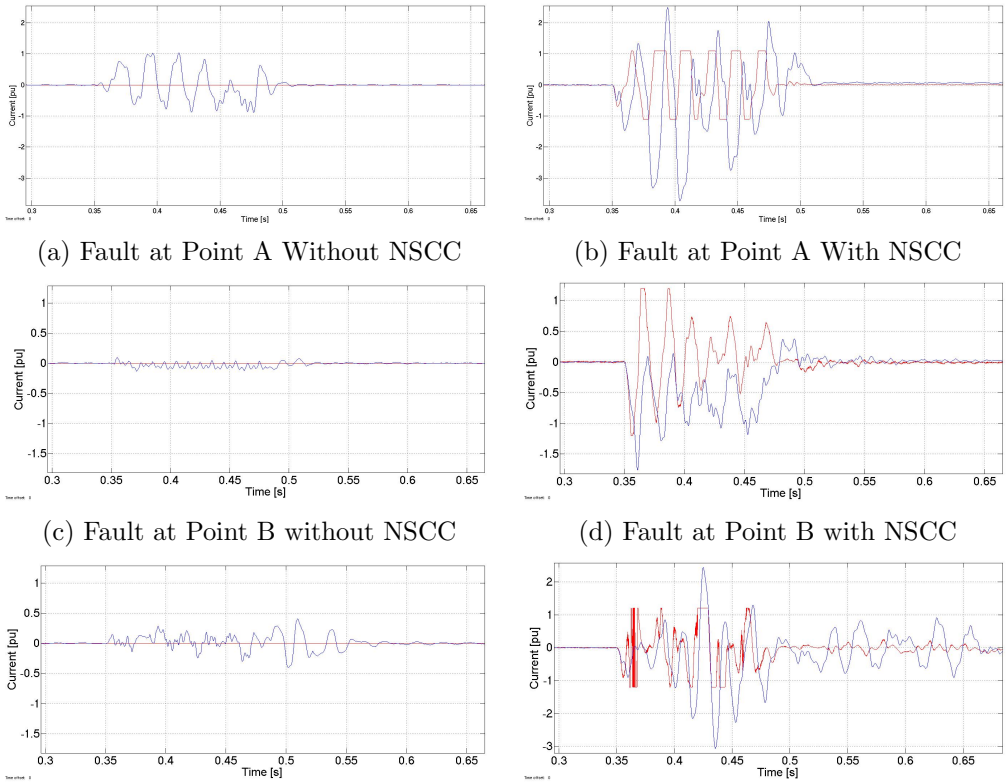

(a) Fault at Point A Without NSCC

(b) Fault at Point A With NSCC

(c) Fault at Point B without NSCC

(d) Fault at Point B with NSCC

(e) Fault at Point C Without NSCC

(f) Fault at Point C With NSCC

Figure 45: D Axis NSC During a DLG fault

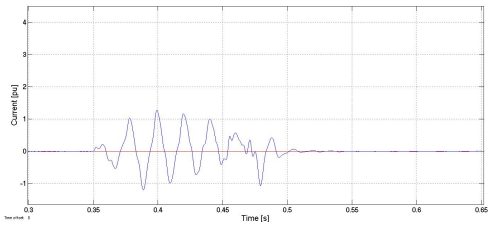

(a) Fault at Point A Without NSCC

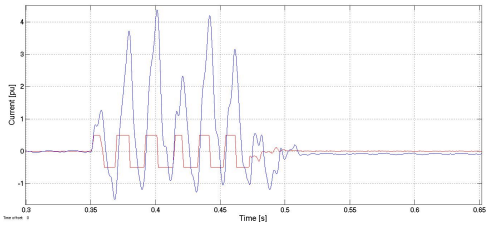

(b) Fault at Point A With NSCC

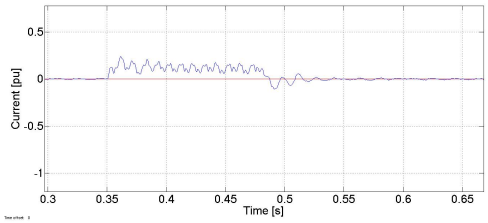

(c) Fault at Point B without NSCC

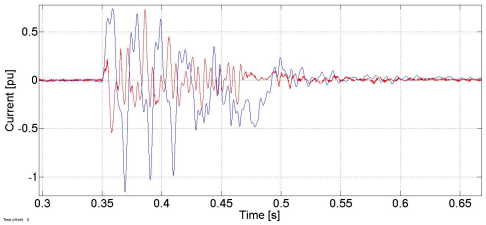

(d) Fault at Point B with NSCC

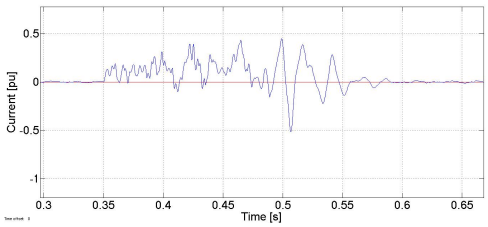

(e) Fault at Point C Without NSCC

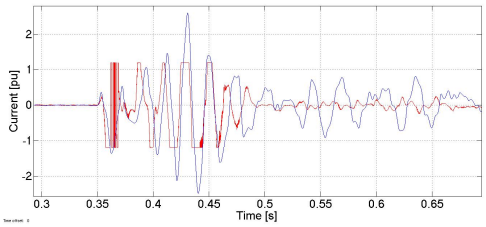

(f) Fault at Point C With NSCC

Figure 46: Q Axis NSC During a DLG fault

5.5 Fault Effects on the WTG Generator Side Converter

The fault effects on the generator is almost negligble. Below the effect on the reference turbine generator side of the converter from a DLG fault at point C is examined and compared to the effect on the aggregated WTG.

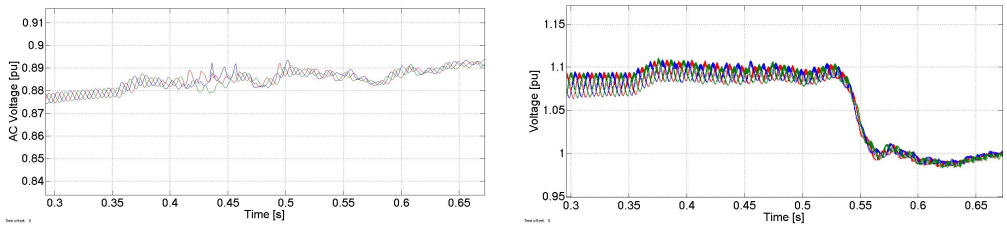

(a) Rms Voltage at the Aggregated WTG

(b) Rms Voltage at the reference turbine

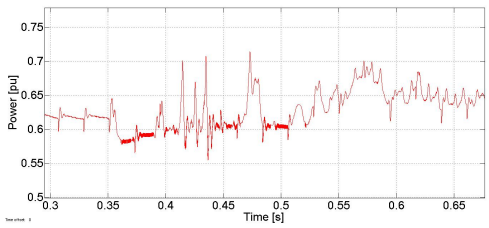

(c) Power from the Aggregated WTG

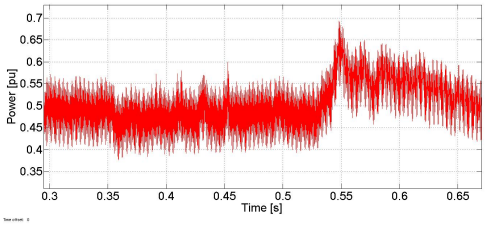

(d) Power from the reference turbine

Figure 47: Power and Rms Voltage at the Stator

From these graphs it can be seen that the voltage at the stator terminals for the reference turbine rises a tiny amount during a fault, whereas the voltage is almost unaffected in the aggregated WTG. The reason for this is that the average model takes the output m_{abc} and multiplies with half the DC voltage to obtain v_c, while the reference turbine outputs v_c directly to the PWM, which is only correct for $U_{DC,pu} = 1$. This can be corrected as explained in chapter 3.1.1. The power signal in the reference turbine showed above is filtered, but still show large oscillations due to the switching action. The graphs show a quite steady output of power, which is expected, since all of the excess power will be fed to the DC chopper. So there is no need to diminsh power production, except for secondary reasons like storing the elecrical energy as rotational energy rather than wasting it in the DC chopper. The little peak after clearing the fault is due to that the DC voltage falls below 1 pu, meaning the AC voltage drops slightly, and more current is fed from the generator.

6 Discussion

The discussion part will examine the results found in the previous section, and analyze what challenges and possible solutions there are, before going in depth in some of the background theory relevant for these challenges and possible solutions.

6.1 Challenges and Possible Solutions

The results obtained show that the NSCC is not working as expected. The main problem seems to be that the system becomes less unable to regulate system parameters quickly and it becomes slightly unstable, when the NSCC is enabled. The reason for this is suspected to be improper tuning of the system controllers. There is a possiblity that there are controllers with competing control objectives present in this thesis, or that some controllers are not quick enough to properly regulate the controller input. Since the NSCC requires sequence seperation, there will be a slight deviation due to the sequence seperation during abrupt changes in current and voltage. However these deviations will disappear in less than 0.01 seconds, and they are unlikely to be the main reason for the slower and slightly unstable control system.

Looking at the way the system behaves when the fault is cleared when the NSCC is enabled, one can see that the HVDC link DC voltage has a large peak. This overshoot could theoretically be decreased by decreasing the controller gain in the inner current control loop. This peak would also be limited by increasing the proportional parameter in the DC voltage controller in the onshore converter. This have been confirmed by experiments, but this also made the rest of the system slightly unstable, and unable to control oscillations in reactive power in the offshore grid, even during balanced network conditions.

This last problem touches on one of the main challenges with this type of controller and computer simulations. The control design is by definition unable to control reactive power oscillations, and the simulations that are performed have the problem that they do not have entirely realistic transient conditions, but very abrupt, loss free, undamped changes, which results in high values, especially since there are swich models and capacitors involved. The problem is probably not made better by the problem with distorted voltage waveforms mentioned in 5.1.

That the challenges mentioned in this section are related to the controller implementation and not the theory behind it, can be tested by simulating an three phase to ground (3PG) fault in the simulation model. This sym-

metrical fault should ideally give equal results with and without NCSS, as the negative sequence current and references should be zero during balanced network conditions.

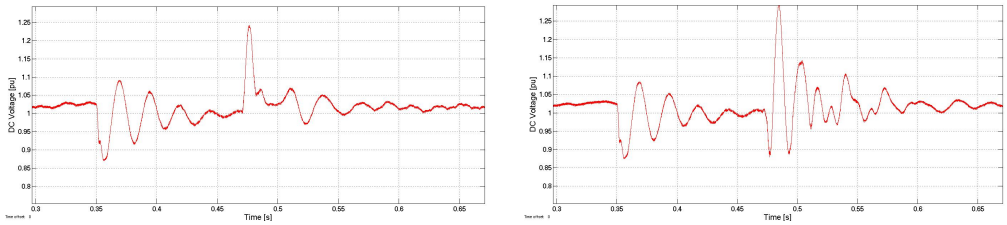

(a) DC Voltage Without NSCC (b) DC Voltage With NSCC

Figure 48: HVDC link DC Voltage during a 3PG Fault

As figure 48 reveals, the NSCC performs less well. The voltage is nearly identical during the fault, but when the fault is cleared at 0.470 s, the NSCC is slower to react to the transient condition when the power flow is reversed, and it performs much worse. The same situation can be seen for i_{dn}, i_{qn}, U_{WTG} and v_x in Appendix E.4. The same situation occurs for some of the faults scenarios in the beginning of the fault period as well. Initially the controller with the NSCC performs worse the first few cycles, but after the fault has been active for some time, the controller manages to control the power oscillations so that the DC voltage oscillations is diminished. This especially true for faults at the HVDC link offshore converter terminals.

It would then seem that the best way to continue would be to create a more detailed and better tuned model. It is suggested to use a more analytical approach to tune the various controllers than the experimental approach used in this master thesis, such as [22] explains for example. Further work should also be done to improve the voltage waveform in the AC offshore grid, as suggested earlier. This might improve the results so that one can see a clear improvement in the DC voltage oscillations by enabling the NSCC.

6.2 Sequence Control

The problem with this type of control system is in part the way the different controllers interact with one other. For instance; the NSCC is tuned to avoid oscillations in active power, while the PSCC are set to control active and reactive power. This means that active power is controlled by two different controllers, which might influence one another, even though they theoretically should not.

The main problem however, is that the controller does not have enough degrees of freedom to fully control the system. [12] and [13] shows how oscillating active and reactive power arises when the system currents and voltages contains both positive and negative sequence components, which can be described by equation 6.1, where the last two terms give rise to oscillations with 2ω frequency in active and reactive power, and therefore also in the DC voltage.

$$\begin{aligned} P &= v * i \\ P &= v_p i_p + v_n i_n + v_p i_n + v_n i_p \end{aligned} \tag{6.1}$$

When written with dq components, this becomes an equation with 24 terms, presented earlier in chapter 3.4.2. Four of these are related to active power, four are related to reactive power, eight are related to oscillations in active power, and eight are related to oscillations in reactive power. The oscillations in active and reactive power can also be split into two groups of four terms in phase with each other, oscillating 90 degrees phase shifted from the other four terms. These two groups of terms can be controlled to cancel each other out, but in order to do so, one degree of controller freedom is required. Since there is four degrees of freedom, two for each sequence where the two degrees of freedom in the PSCC are used for controlling active and reactive power, there are two degrees of freedom to few to control the entire system. This leads to a underdetermined system where reactive power uncontrolled and free to oscillate.

For various situations, different control objectives might be advantegeous, as described in section 3.4.2. The control method chosen in these thesis is to cancel active power oscillations. This option leaves the systems reactive power free to oscillate. When $Q_{2\omega}$ is a free system parameter, the NSCC must be controlled in such a way that it quickly reaches stable operating conditions during transients. As of this moment, the NSCC in the SIMULINK model is not adequately tuned. The reative power oscillations do damp out when the controller have had some time to adjust, but this should be a much quicker adjustment, as figure 49b shows. Here we can see that oscillations in reactive power continues for quite some time both after the system start-up and after the fault is cleared. This can also be seen in figure 49a where the negative sequence voltage reference is shown. That the reactive power oscillations are present so long in this system might affect the stability of the positive sequence reatctive power controller. When the system model was constructed, the last big challenge before the system was working as intended, was tuning the reactive power controller. The controller was stable

and quick when the NSCC was disabled, but when the NSCC was enabled, the whole system became completely unstable.

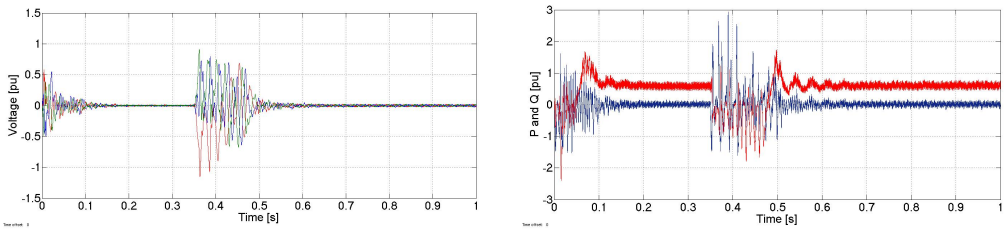

(a) Negative Sequence Voltage Reference (b) P and Q During the Simulation Run

Figure 49: Relation Between Reactive Power Oscillations and NSCC Output Reference

What becomes evident is that it is desireable to control reactive power oscillations in the system, but that this is not possible with the current control strategy. Theoretically the oscillations should not become a large problem, but possibly due to poorly tuned controllers and very distorted waveforms in the AC offshore grid, it does becomes problematic. However, it is possible to control both active and reactive power oscillations, but a trade off must be made on how much of each that can be controlled. Should further tuning of the control system proposed in this thesis show that the control system is unable to meet the required demands, it is recommended that one looks into how to create a controller that will use NSCC references to partly control active, and partly reactive, power oscillations to be zero.

It is also worth to mention that during a short circuit at the converter terminals of a WTG, the NSCC significantly degrades the situation in the b2b converter as it hinders power delivery to the grid, resulting in higher DC voltage during a fault. A way to counteract this is to have a control system that switches control strategy when the amount of negative sequence current passes a threshold, to either a control method that has the objective to limit zero sequence current, or to transmit the maximum amount of active power, called Instantaneously Controlled Positive-Sequence and Instantaneous Active Reactive Control respectively in [12]. To implement this control system and to decide which strategy would be the best will have to be a topic of further work.

A quick check was done in order to verify that other NSC references could be applied to the NSCC, and below the results of a DLG fault at point B with NSC references equal to zero is presented. The results are similar to the compared standard controller, but the median DC voltage is lower when zero NSC references are used. Other measurments from this test can be found in

the Appendix E.5

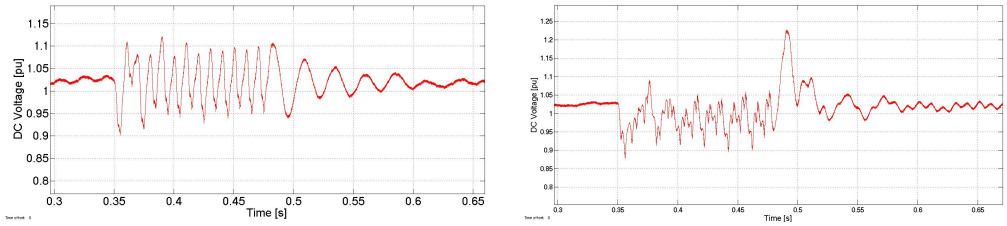

(a) Fault at Point B without NSCC (b) Fault at Point B with NSCC

Figure 50: HVDC Link Voltage During a DLG fault

An important part of veryfying the theory of limiting DC overvoltages with negative sequence current injection (NSCI), is that the HVDC link offshore converter also should use this method. The power transfer from this converter will not be limited in the same way during a fault, since power flow is under normal operating conditions in the opposite direction of the injected NSC. [6] shows that the biggest effect from NSCI is due to the HVDC link offshore converter. The simulation model in this thesis has a NSCC implemented in the HVDC link offshore converter, but it has been disabled due to stability issues. If the challenges in regard to tuning and voltage waveforms are solved, this controller might also be implemented.

Another problem with this type of control philosophy is highlighted in [23]. In order for this control system to work effectively, it is dependent on quick and precise seperation of the sequence signals. The SOGI QSG is relatively fast and efficient, responsive down to a quarter of a cycle, or 5 ms, but it is of course not perfect. The system is also dependent on removing 100 Hz oscillations from signals used to generate the current references. This means that the positive sequence DC voltage controller must have oscillation free DC voltage and DC current as input. In order to achieve this in the simulation model, notch filters have been used, as desribed in chapter 4.1.5. The response of the notch filters were not completly satisfying, and a source of system improvement would be to implement better tuned notch filters in order to have oscillation free DC voltage and DC current.

7 Conclusions and Further Work

7.1 Conclusions

This thesis has looked into the effects of unbalanced faults in the AC grid in an offshore wind farm. In addition to changing the power flow in the wind farm and causing high over currents, these faults creates negative sequence currents and voltages that flow in the system causing active and reactive power oscillations. The active power oscillations will transfer to the HVDC link through the converters, causing voltage oscillations in the HVDC link DC voltage.

This thesis has tested out a negative sequence current controller to see whether negative sequence current can be injected into the offshore AC grid in order to control the active power oscillations, and thereby also the HVDC link DC voltage oscillations, to be zero. In theory this should be possible, and other sources have confirmed this([6], [24] and [25]). The applied method for testing have been to construct a model of an offshore wind farm with VSC based HVDC link technology and wind turbines with full scale converters. In addition to the physical components a control system have been built, including a negative sequence current controller that can be enabled and disabled in order to perform tests to research the impact of this controller compared to the standard controller. In most cases tested in this thesis, the negative sequence current controller did not improve the HVDC link or wind turbine converter DC voltage oscillations. The exception was a DLG fault at the offshore HVDC link converter terminals, which showed a slight improvement. Other cases had an improved waveform for a short period of time after the fault had been active for some cycles, and before the fault was cleared.

The control system built to test this theory is functional, but it suffers from inadequate control parameter tuning. Moreover the quality of the AC voltage in the offshore grid is of such a low quality that it might affect the results negatively. A symmetrical three phase fault was also simulated on the system. In theory this should give an equal result with and without the negative sequence current controller, but the controller clearly that it performed worse than the standard controller. Therefore one can conclude that the problem is the implementation of the negative sequence current controller, not the theory behind the working method of the controller.

One of the greatest challenges with this type of control is that it leaves reactive power free to oscillate, while at the same time causing slight disturbances during transient conditions. When combined with the aforementioned problems, this creates a difficult task for the control system in the simula-

tion model. A solution might be to construct a controller that is able to partially control oscillating active power and partially control oscillating reactive power. However, adequate control parameter tuning and a system with more extensive filtering, combined with an enabled negative sequence current controller in the offshore HVDC link converter might prove enough to confirm the theory presented in this master degree.

7.2 Further work

The following work is recommended to be carried out:

- Improve the simulation model with regards to the offshore AC voltage quality.
- Perform a more thorough and analytical control parameter tuning for the system control parameters.
- Implement a better notch filter or a higher order filter to remove negative sequence components from the signals used for the generation of positive sequence current controller references
- Enable the HVDC link offshore converter negative sequence current controller and repeat the tests performed in this thesis
- Create an addition to the controller in the wind turbines that switches control strategy during faults with high negative sequence currents.
- Compare the advantages and disadvantages of using a PR controller in stead of a PI controller and dq coordinates.
- Research the possibility to create a controller that controls partially reactive and active power oscillations.
- Change the voltage levels in the model to more realistic levels and provide more detailed data for the physical components in the system.
- Perform tests to see whether a negative sequence current controller implemented in the onshore HVDC link converter can be used to help the offshore wind farm in passing the grid code requirements.
- Update the generator data and control system and in the NOWITECH reference turbine to more realistic values.
- Perform research on the effects on the NOWITECH reference turbine in terms of acceleration and turbine voltage during faults.

A Tips for Running SIMULINK Simulations on Large Projects

This section will try to give an insight in challenges and pitfalls when creating a SIMULINK model of this size and complexity. The motivation is that students often has limited knowledge and experience with running more extensive simulations in Matlab Simulink. This section does not aim to give an introduction in how to performe large projects, but rather to list some challenges and reflections regarding SIMULINK that could save a lot of time if they are considered.

A.1 Set-Up

When setting up the model, it is important to know which components to use, why to use them and not other alternatives, and how to set the values in these components. A quick mistake to make is to grab the first block that one assumes is correct, putting in a value on assumes is sensible, and to try to run the model. The model will perhaps run, and maybe even run with results close to what you would expect, but there might be latent issues that will surface later when you increase the complexity of the system.

A quick example would be the "Capacitor" block used to stabilize voltage in the HVDC link. The capacitance is set from the following formula:

$$\tau_C = \frac{\frac{1}{2}Cv^2}{P_n} \tag{A.1}$$

Where the time constant should be in the range of 5-20 milli seconds. If the capcitor value is set to small, the voltage at the converter terminals will not stabilize, and the AC voltage will also be unstable, it it is too big, the DC voltage will stay constant no matter what you do.

Moreover, using the per unit system generally makes it easier to give sensible values to the system parameters. An example could be the reactor inductance, which should be in the order of 0.10 to 0.20 pu. The per unit system has some pitfalls however, more on this later.

During the initial phase of building the model, one should also consider using the simplest form of the model. When one has understood well how this functions, one can increase the complexity of the system. It might be a good decision to implement an average model of the converter before trying to build a switched model. In this fasion, one would avoid some of the challenges related to the switched models so one can focus on the central areas of converter operations. If one finds a complex suggestion for a control

system in an article, one should wait some time before trying to implement it. It might be very time consuming to try to make a complex control system work, only to discover later that a simpler and quicker solution would have sufficed.

A.2 Modularity

When constructing large models, it is very difficult to gradually build on one big model because: it becomes difficult to look for errors in a large system; it becomes difficult to see which components are important and not; and it is easy to loose sight of what the individual components are meant to do. The solution is to build and test parts of the system separetly, and to integrate them when one are certain that they are working correctly. The time required for this type of work style may seem more demanding, but in the end it might be more efficient. The model used in this thesis is for example made up of four converters, which are tested in isolation before they were installed together.

A.3 M-scripts and pu Systems

When the system becomes large, a very common mistake to make is to decide to change one system parameter to optimize the model, and then forget to change all related parameters that will be affected by this change. A typical example would be changing the inductance in the converter reactor, without changing the time constant of the VCC, which is closely related to this value. The way to avoid this is to be consistent in using workspace variables to set variable values in the system. When changing a variable, all related variables are then set by a formula including the changed variable as a parameter, and they are then automatically updated. Another thing to consider when using this approach is that it might be advantegeous to use different variables for components that are built and tested in different modules. So even though the per unit value of inductance is the same for three different converters, it might be smart to create three different variables for these inductances. The reason for this is that one might do changes later that involves changing just one of these values, and then it becomes an ordeal to locate all variables that one must change. Furthermore, when tuning the controllers of one converter, one should leave the other converters unaffected.

The per unit system is very usefull in making sure that one have sensible values for the various parameters in the system, but it is easy to make mistakes if the system architecture is not thoroughly understood. When one first are constructing the system, it might therefore be constructive not to

use the per unit system in the controller system, as the abstraction level becomes higher.

A.4 Troubleshooting

The first tips for avoiding long and tiresome troubleshooting sessions is to have a clean and tidy model. Furthermore, testing models separetly to see if they behave as suspected is easier than testing the full system. And most imporatantly: Simplify the model that is under testing when the fault is not found. For instance when testing a converter, a step in simplifying the test model might be to use a constant DC source on the converter DC terminals, so that one are certain that the problem is not oscillating or unstable DC voltage. Or to remove cable models and transformers and use resistances and inductances in stead or to connect an stiff voltage source next to the converter reactor. Then one can eliminate different sources of possible errors.

Another source of error when one has put together several modules, is that the control strategy might be incoherent. Check that:

- It should be only one source that can set the AC voltage angle. This can be a stiff grid, a converter with a PR controller or a converter with a reference angle.
- That no two converter controllers are trying to control the same variable, i.e. to have two controllers connected by an AC network that both control reactive power injection into the grid. These two controllers might then have competing controller objectives.

Another common mistake is to have wrong sign on controller or measurment blocks. A method of making this less likely to be an issue, it to create a convention of power direction, for instance that power is always flowing into the converter.

A.5 Matlab Problems

Matlab SIMUNLINK has some unusual methods of working that are relevant when modelling converters. The first is that the "Park Transformation" block does not use the same variant of the transformation one most commonly finds in litterature. Furthermore, the "3 Phase PLL" block does not lock the angle to the phase A voltage, but it is shifted 90 degrees from it. Using these two blocks together will result in a system that is behaving as expected, but should one of the blocks be exchanged by a block that the user has made on his own, the system will be malfunctioning. But always examine "ready

made" SIMULINK blocks by pressing ctrl+u to see what they are actually doing, it might be different to what one expected.

A.6 Numerical Issues

Starting a simulation in MATLAB SIMULINK might be difficult. There can be controllers that are controlling a variable they need input from to control, creating an algebraic loop. Solving this algebraic loop might be done by eliminating it all together, setting sensible initial conditions in integrator blocks, or creating small delays in the system input, for instance a discrete "Delay" block found in the SIMULINK library [26]. In the worst cases, this will not work. Then a possibility could be to create a logical condition that has the purpose of bypassing the controller for a moment of time, such as the length of the first 5 dicrete timesteps.

Some numerical errors might be because the timestep in the simulated model are too high, so that required information is lost due to low timeframe resolution. The maximum timestep should be in the order of 10 smaller than the time required for a switching cycle.

A.7 Control Philosophies

When implementing a control philosophy, it is important to see how many degrees of freedom one has, and which parameters one wish to control with these degrees. Listing the required variables to be controlled and which controller that should control which variable could be beneficial in order to be able to keep an overview over the system.

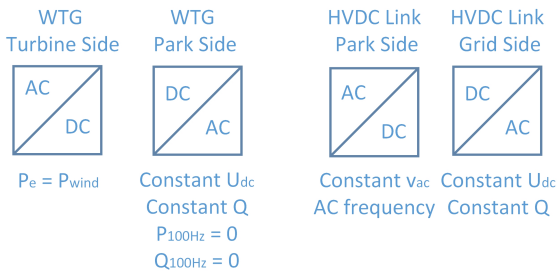

Figure 51: Control Philosophy of the Modelled System

It is also important to be careful when one are using several sources of information when building a control system. One article may use methods that are noncompatible with another system, and another might use a control

system that are dependent on some properties of another part of the system that one did not intended to use. The best method of making sure that one has understood and considered all parts of the system one intend to build, is to write about the theory applied in the system while building it in SIMULINK.

A.8 Summary

The tips given in this section can be summed up into the following advice, which can be quite the timesaver:

- Build the system slowly and in small parts that are easy to have good overview over.
- Be consistent and specific when using variables, create a M file that contains all system parameters.
- When the smaller parts should be integrated, make sure that the control philosophy is consistent and that the background theory is well understood.
- When troubleshooting, start to break up the system in smaller parts and troubleshoot on these. If the fault is not found, simplify the system so that only the relevant parameters are left.
- Make certain that "ready made" blocks from the SIMULINK library work as required.
- If there is no solutions after this, check for numerical problems such as: too large simulation time step; algebraic loops; initial values in integrators, capacitors and so forth; and that the correct solver is used.

B Turbine Data

The data for the generator is taken as standard values found in Matlab SIMULINK. For further research, it is recommended that more specific data from the reference turbine specification is used in order to have results closer to reality. The data is presented below in pu:

$$\begin{aligned} R_s &= 2.85\ 10^{-3} & R_{kd} &= 0.0652 \\ L_l &= 0.1 & L_{lkd} &= 0.5134 \\ L_{md} &= 0.5 & R_{kq1} &= 0.0287 \\ L_{mq} &= 0.4 & L_{lkq1} &= 0.2553 \\ R_f &= 5\ 10^{-3} & R_{kq2} &= 7.765\ 10^{-3} \\ L_{lfd} &= 0.1 & R_{lkq2} &= 0.9167 \end{aligned}$$

Rated rotational speed is 13.5 rpm. If the grid frequency is desired to be approximately 50 Hz, this means that the polepairs is set to:

$$\begin{aligned} p &= 250\ pairs \\ f_n &= 56.25Hz \end{aligned} \tag{B.1}$$

From figure 52 the inertia constant J can be estimated, and from it; the time constant H used in the SIMULINK model. This is done by creating 10 small lumped masses at intervalls of 0.1, centered at the middle of these intervalls. This gives:

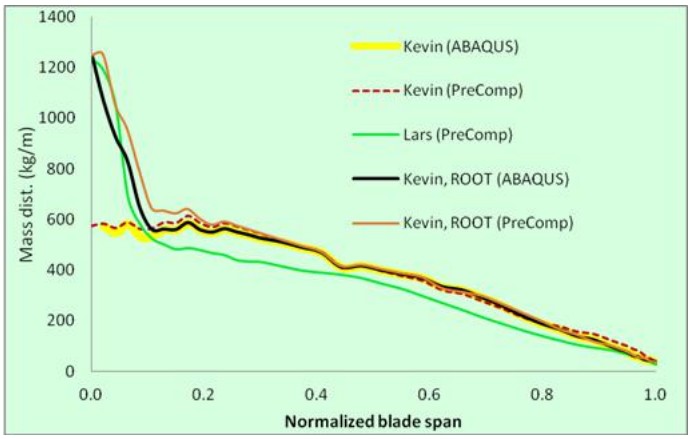

Figure 52: Blade Mass vs Radius

$$M = m_1 + m_2 + ... + m_{10} \tag{B.2}$$
$$M = 0.1R[\frac{1200-600}{2} + 600 + \frac{600-600}{2} + 600 + ...$$
$$... + \frac{150-50}{2} + 50]$$

Moment of inertia for a thin rod is given by:

$$I = \frac{mL^2}{3} \tag{B.3}$$

When considering a turbine with three blades, and using the blade mass graph presented above, one can create small lumped masses with 0.1 distance between them and integrate to find the total moment of inertia J.

$$J = 3R^2[\frac{m_1 * 0.05^2}{3} + \frac{m_1 * 0.15^2}{3} + ... + \frac{m_{10} * 0.95^2}{3}]$$
$$H = \frac{J}{\frac{1}{2}\omega^2 S_n} = 2.65s \tag{B.4}$$

C PU System

The control in this project have been implemented in pu. Basic relations is established in this appendix.

$$
\begin{aligned}
&V_{n,phase-phase,rms} = 132kV \\
&P_n = 900MW \\
&pf = 0.9 \\
&S_n = 1000MW \\
&I_{n,rms} = 4.37kA \\
&Z_n = \frac{V_n^2}{S_n} = 17.42\Omega \\
\\
&V_d = \sqrt{2/3}V_n \\
&I_d = \sqrt{2}I_n \\
&Z_d = Z_n \\
&S_d = \frac{2}{3} \\
\\
&S_{DC} = S_n \\
&I_{DC} = \frac{3\sqrt{2}}{4}I_n \\
&Z_{DC} = \frac{8}{3}Z_n
\end{aligned}
\tag{C.1}
$$

D Tuning of the Controllers

The tuning of the controllers in the SIMULINK model have been configured partly experimentally, and partly by analytical means described in [6], [7] and [9].

D.1 Inner Current Loop:

The tuning of the inner current loop PI controller is done by modulus optimum requirement.

The process pole to be canceled is the physical system transfer function showed in figure 6:

$$H = \frac{\frac{1}{R_{pu}}}{1 + \frac{L_{pu}}{R_{pu}s}} \tag{D.1}$$

And the transfer function of the PI controller is:

$$H = \frac{K_p(1 + T_i s)}{T_i s} \tag{D.2}$$

Which gives:

$$T_i = \frac{L_{pu}}{R_{pu}} \tag{D.3}$$

If one consideres the time delay for the converter, which would be equal to the inverse of the switching frequency, one can write:

$$K_p = L_{pu} f_s \tag{D.4}$$

D.2 Outer Control Loops

For the outer control loops, the inner current control loop is considered a time delay, which the outer controller must cancel with its integral controller giving:

$$T_{i,2} = T_{eq} a^2 = (T_i + T_i + T_s) a^2 \tag{D.5}$$

Here a is a freedom in the controller, chosen to be 2. a can vary between 2 and 3, where a lower value results in a more aggresive controller. Considering

the relation between current out of the converter and DC voltage, it can be shown that K_{pDC} for the DC voltage controller is given by:

$$K_{pDC} = \frac{C_{pu}}{a\ T_{eq}} \tag{D.6}$$

And by considering the relation between current out of the converter and reactive power, it can be shown [6] that K_{pQ} for the reactive power controller is given by:

$$K_{pQ} = \frac{\omega_{c,Q} 2 T_{eq}}{3} \tag{D.7}$$

Where $\omega_{c,Q}$ is the bandwidth. Similarily one can consider the relation between current out of the converter and voltage over the filter capacitor, and it can be shown that K_{pAC} for the AC voltage controller is given by:

$$K_{pAC} = \omega_{c,AC} T_{eq} f_s C_{f,pu} \tag{D.8}$$

Where f_s is the switching frequency, $\omega_{c,AC}$ is the bandwidth and $C_{f,pu}$ is the pu value of the filter capacitor.

The proportional constant $K_{p,Pe}$ electrical power regulator in the WTG was tuned experimentally. Since the inertia must be accounted for in the response time of the turbine, a new value for T_{eq} must be computed:

$$T_{i,Pe} = (Teq + H)a^2 \tag{D.9}$$

The table below gives an overview over the theoretical and actual values for all the controll parameters for the systems PI controllers.

Controller	Theoretical Value		Used Value	
	Kp	Ti	Kp	Ti
HVDC Link PSCC VCC	0.9311	0.0477	0.9311	0.0621
WTG PSCC VCC	0.7162	0.0637	0.5730	0.0828
WTG NSCC VCC	0.7162	0.0637	0.5730	1.6552
HVDC Link U_{dc}	11.4338	0.3830	10.5608	0.4976
WTG U_{dc}	12.3120	0.5103	1.1844	0.4976
HVDC Link Q	4.8129	0.3830	6.2529	0.4976
WTG Q	57.7160	0.5103	9.3745	0.4976
V_{ac}	0.5745	0.3830	0.7464	0.4976
P_e			13.7991	11.0976

Figure 53: Table of Controller Parameters for the Simulation Model

E Complete Simulation Results

The following section includes the results from all the faults scenarios. SLG, DL and DLG faults have been applied at point A, B and C, with the exception of a SLG fault at point B. This has almost no effect on the system, as the transformers are not grounded on both sides, and it has therefore been left out. The results also includes a 3PG fault at point B, and the results from a DLG fault at point B with a different NSCC that uses NSC reference equal to zero.

E.1 Fault Effects During a SLG Fault

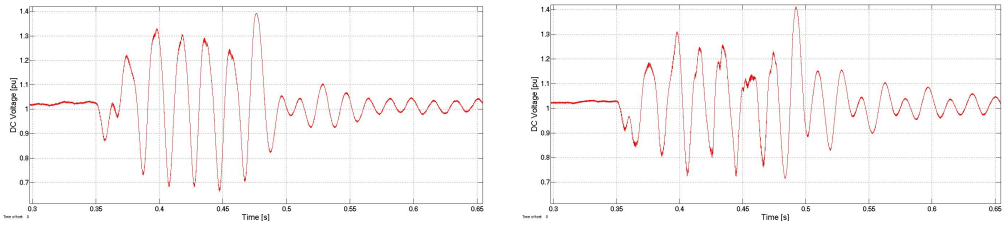

(a) Fault at Point C Without NSCC (b) Fault at Point C With NSCC

Figure 54: HVDC Link DC Voltage During a SLG Fault

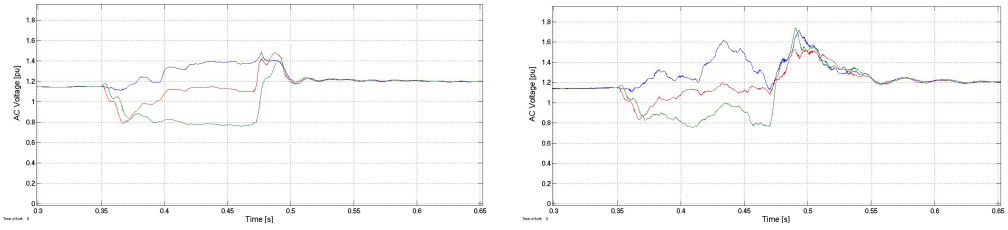

(a) Fault at Point C Without NSCC (b) Fault at Point C With NSCC

Figure 55: Offshore AC Grid Voltage During a SLG Fault

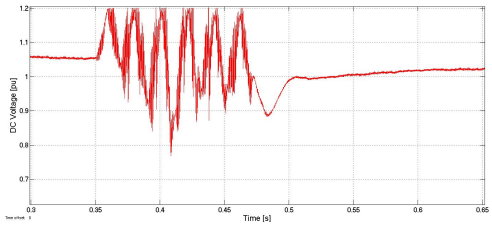

(a) Fault at Point A Without NSCC

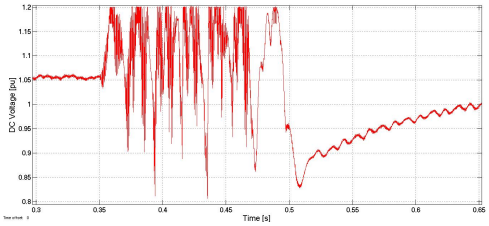

(b) Fault at Point A With NSCC

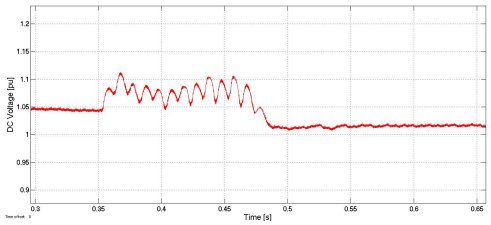

(c) Fault at Point C Without NSCC

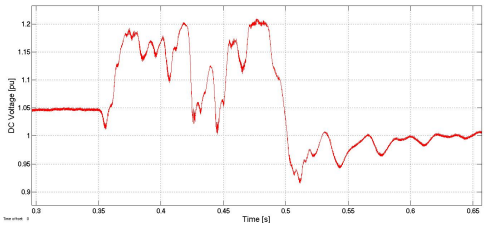

(d) Fault at Point C With NSCC

Figure 56: WTG DC Voltage During a SLG Fault

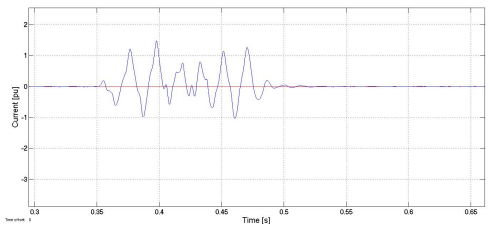

(a) Fault at Point A Without NSCC

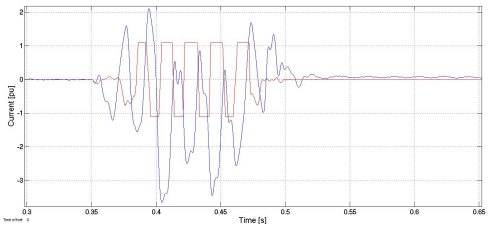

(b) Fault at Point A With NSCC

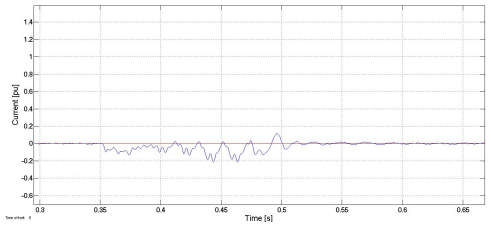

(c) Fault at Point C Without NSCC

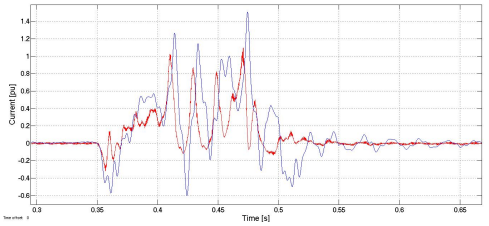

(d) Fault at Point C With NSCC

Figure 57: D Axis NSC During a SLG Fault

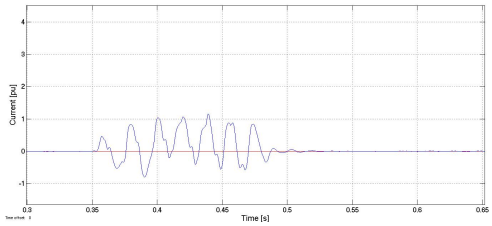

(a) Fault at Point A Without NSCC

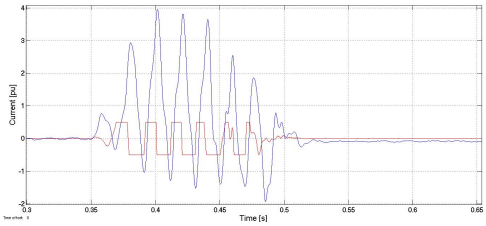

(b) Fault at Point A With NSCC

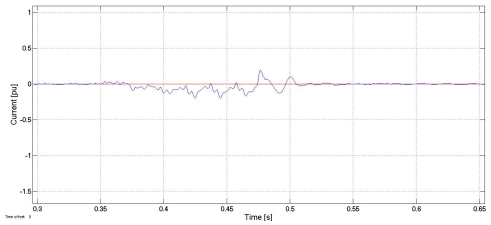

(c) Fault at Point C Without NSCC

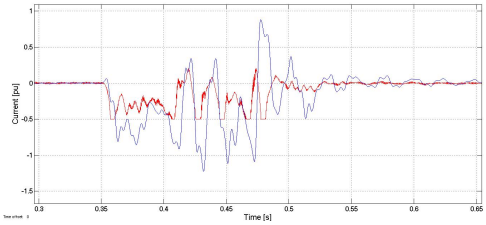

(d) Fault at Point C With NSCC

Figure 58: Q Axis NSC During a SLG Fault

E.2 Fault Effects During a DL Fault

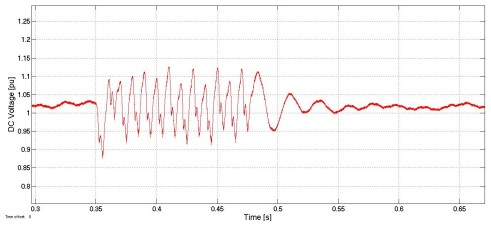

(a) Fault at Point B without NSCC

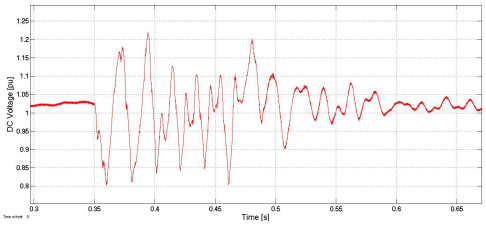

(b) Fault at Point B with NSCC

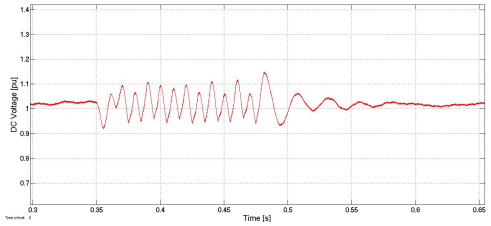

(c) Fault at Point C Without NSCC

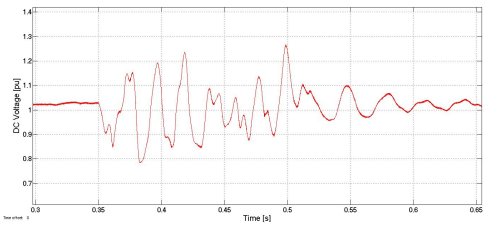

(d) Fault at Point C With NSCC

Figure 59: HVDC Link DC Voltage During a DL Fault

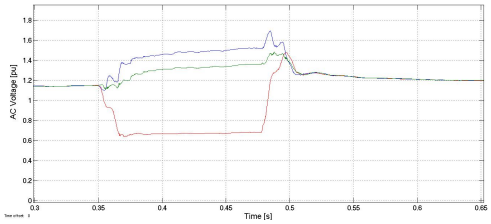

(a) Fault at Point B without NSCC

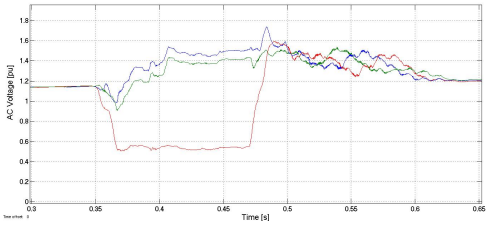

(b) Fault at Point B with NSCC

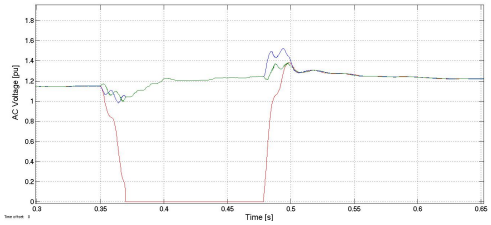

(c) Fault at Point C Without NSCC

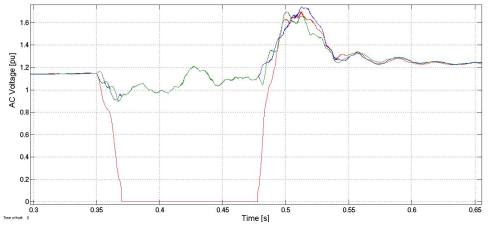

(d) Fault at Point C With NSCC

Figure 60: Offshore AC Grid Voltage During a DL Fault

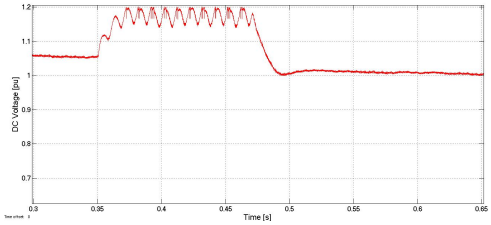

(a) Fault at Point A Without NSCC

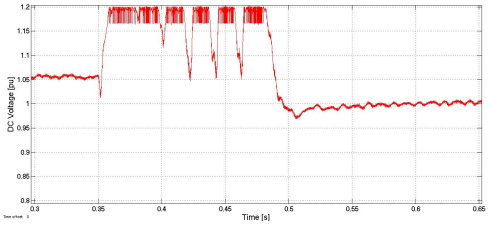

(b) Fault at Point A With NSCC

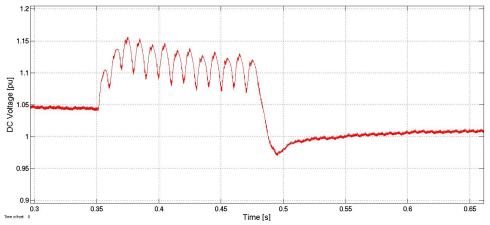

(c) Fault at Point B without NSCC

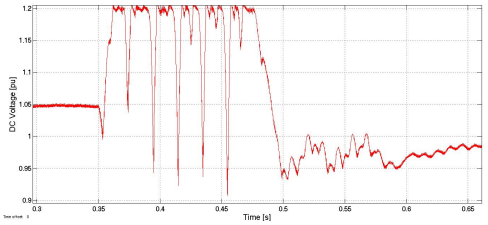

(d) Fault at Point B with NSCC

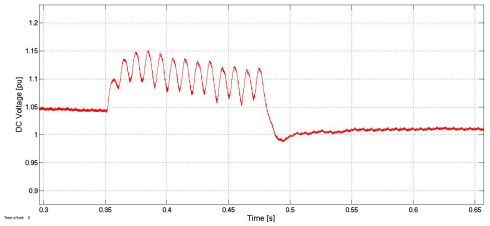

(e) Fault at Point C Without NSCC

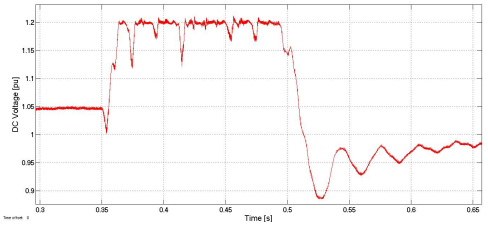

(f) Fault at Point C With NSCC

Figure 61: WTG DC Voltage During a DL Fault

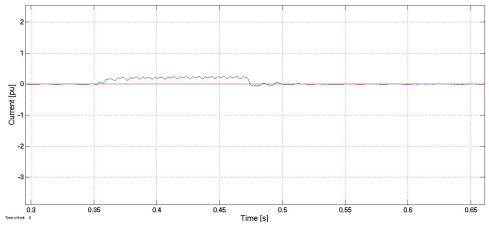

(a) Fault at Point A Without NSCC

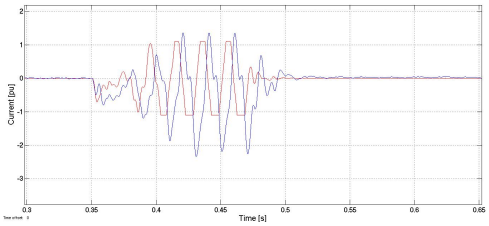

(b) Fault at Point A With NSCC

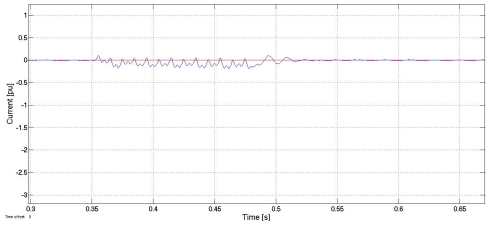

(c) Fault at Point B without NSCC

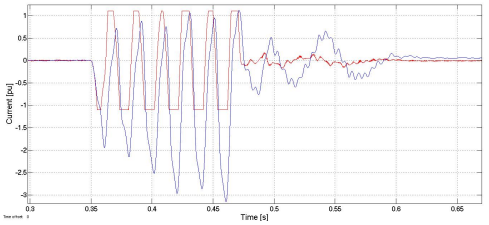

(d) Fault at Point B with NSCC

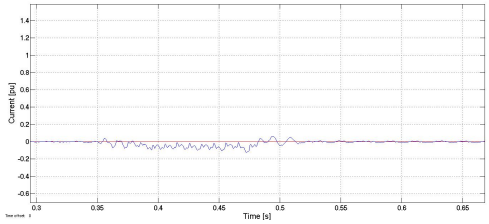

(e) Fault at Point C Without NSCC

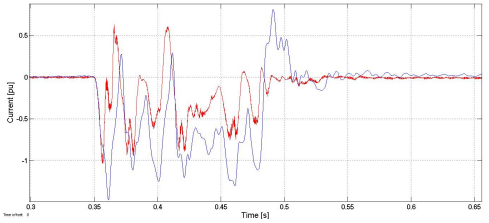

(f) Fault at Point C With NSCC

Figure 62: D Axis NSC During a DL Fault

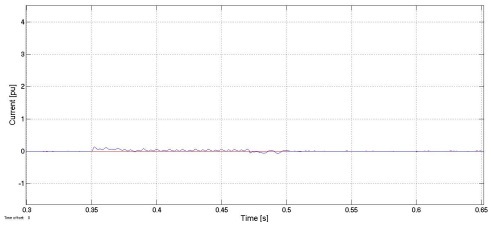

(a) Fault at Point A Without NSCC

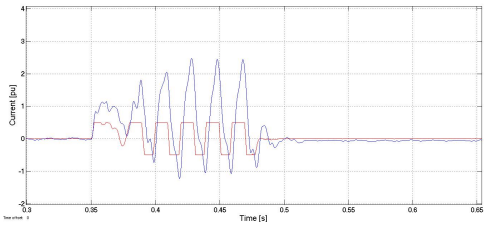

(b) Fault at Point A With NSCC

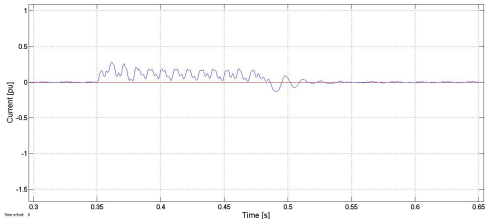

(c) Fault at Point B without NSCC

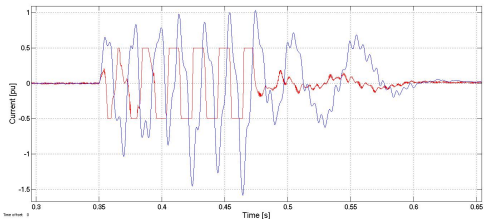

(d) Fault at Point B with NSCC

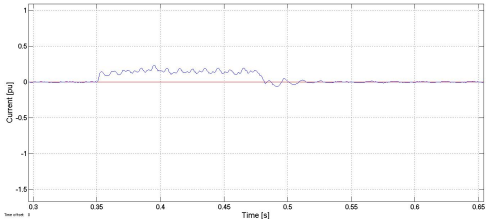

(e) Fault at Point C Without NSCC

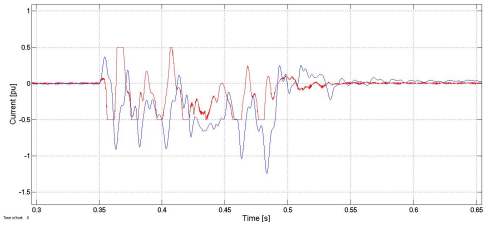

(f) Fault at Point C With NSCC

Figure 63: Q Axis NSC During a DL Fault

E.3 Fault Effects During a DLG Fault

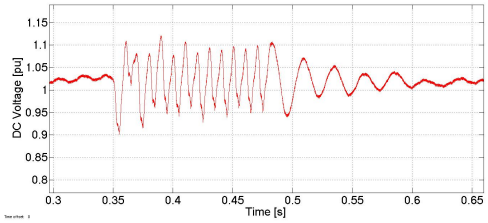

(a) Fault at Point B without NSCC

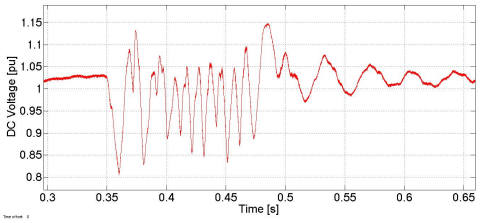

(b) Fault at Point B with NSCC

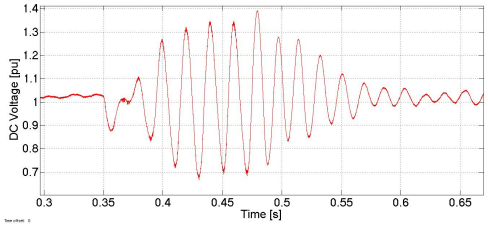

(c) Fault at Point C Without NSCC

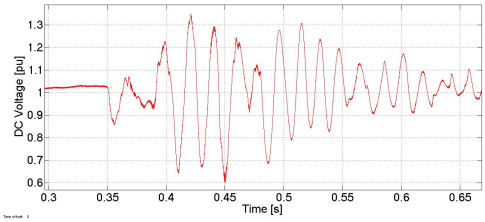

(d) Fault at Point C With NSCC

Figure 64: HVDC Link DC Voltage During a DLG Fault

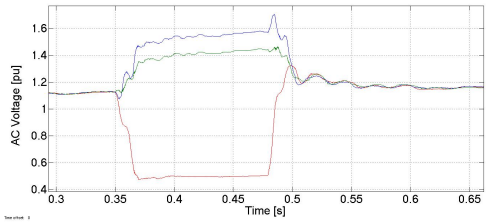

(a) Fault at Point B without NSCC

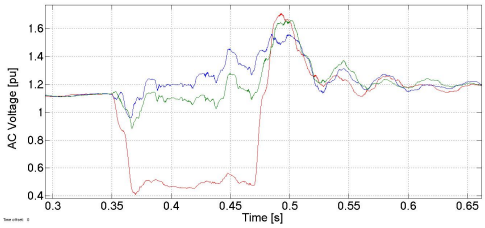

(b) Fault at Point B with NSCC

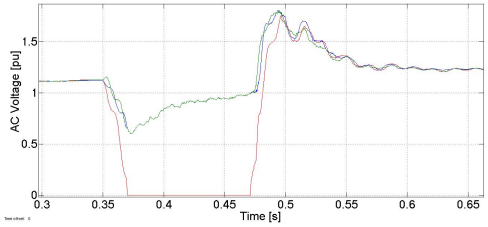

(c) Fault at Point C Without NSCC

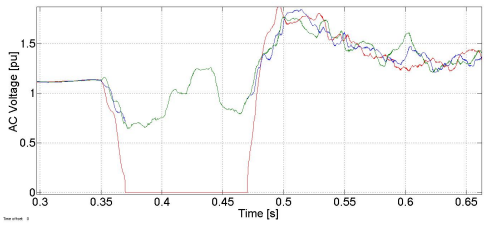

(d) Fault at Point C With NSCC

Figure 65: Offshore AC Grid Voltage During a DLG Fault

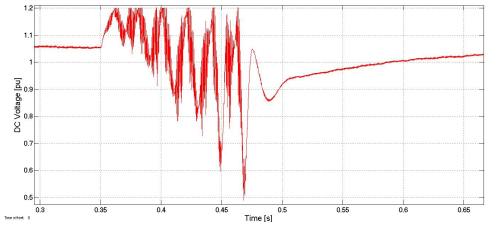

(a) Fault at Point A Without NSCC

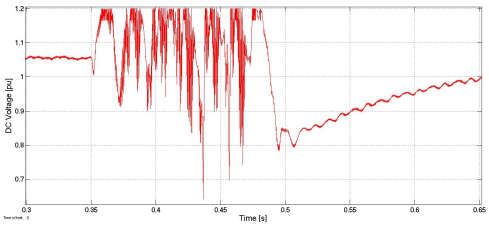

(b) Fault at Point A With NSCC

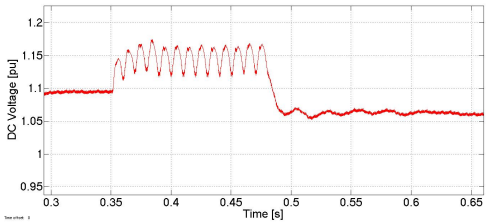

(c) Fault at Point B without NSCC

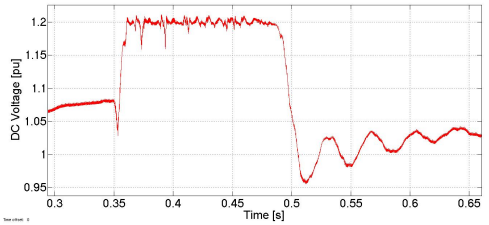

(d) Fault at Point B with NSCC

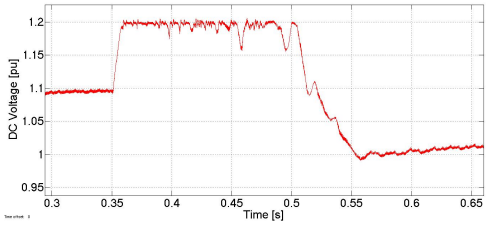

(e) Fault at Point C Without NSCC

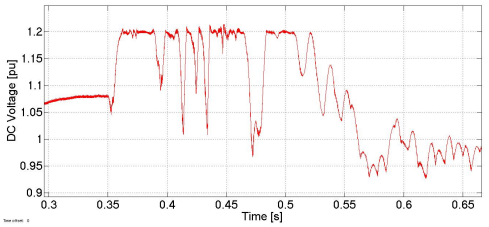

(f) Fault at Point C With NSCC

Figure 66: WTG DC Voltage During a DLG Fault

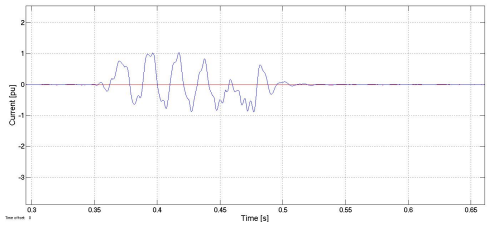

(a) Fault at Point A Without NSCC

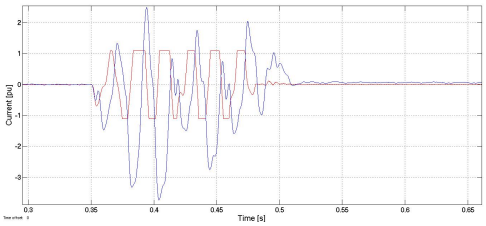

(b) Fault at Point A With NSCC

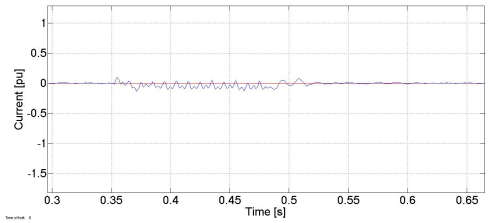

(c) Fault at Point B without NSCC

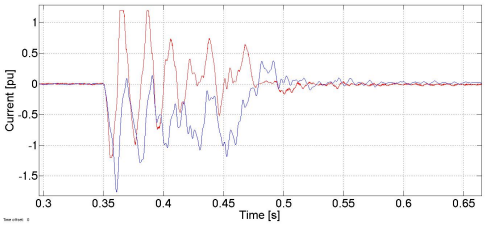

(d) Fault at Point B with NSCC

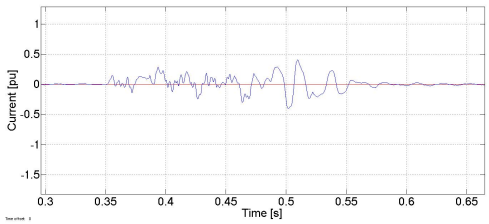

(e) Fault at Point C Without NSCC

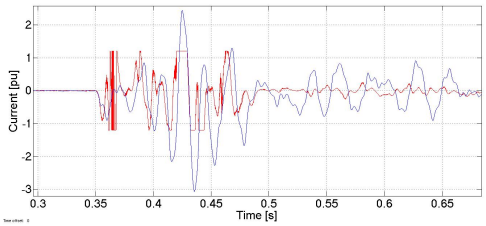

(f) Fault at Point C With NSCC

Figure 67: D Axis NSC During a DLG Fault

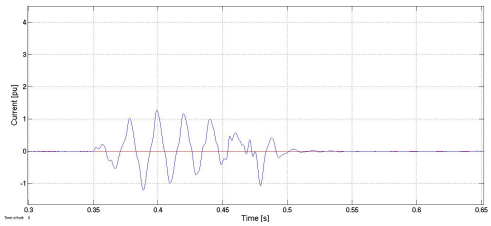

(a) Fault at Point A Without NSCC

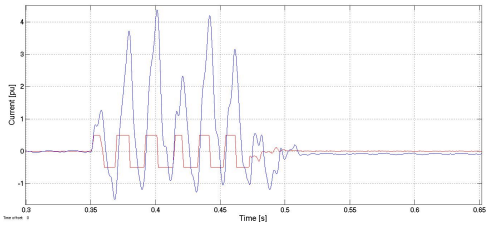

(b) Fault at Point A With NSCC

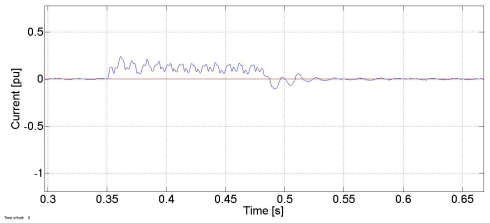

(c) Fault at Point B without NSCC

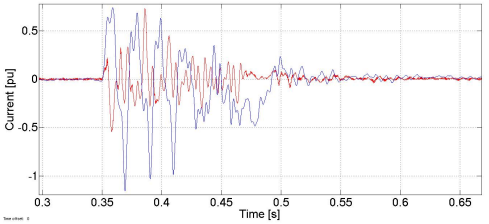

(d) Fault at Point B with NSCC

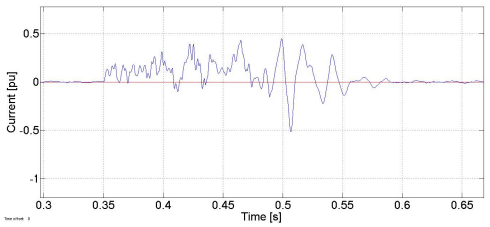

(e) Fault at Point C Without NSCC

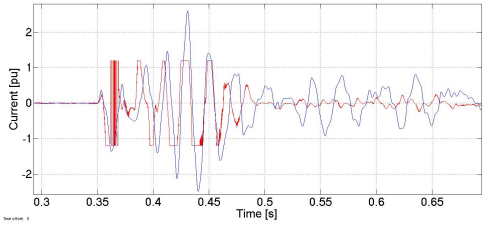

(f) Fault at Point C With NSCC

Figure 68: Q Axis NSC During a DLG Fault

E.4 Fault Effects During a 3PG Fault

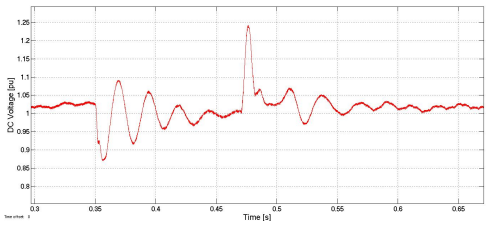

(a) Fault at Point B without NSCC

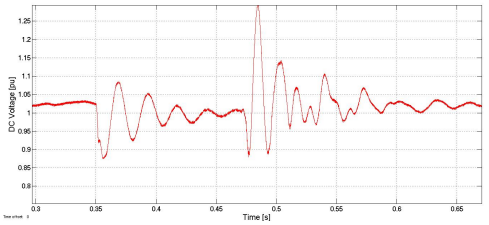

(b) Fault at Point B with NSCC

Figure 69: HVDC Link DC Voltage During a 3PG Fault

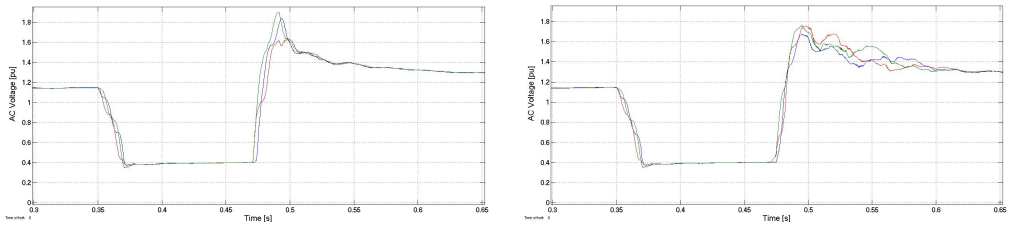

(a) Fault at Point B without NSCC (b) Fault at Point B with NSCC

Figure 70: Offshore Grid AC Voltage During a 3PG Fault

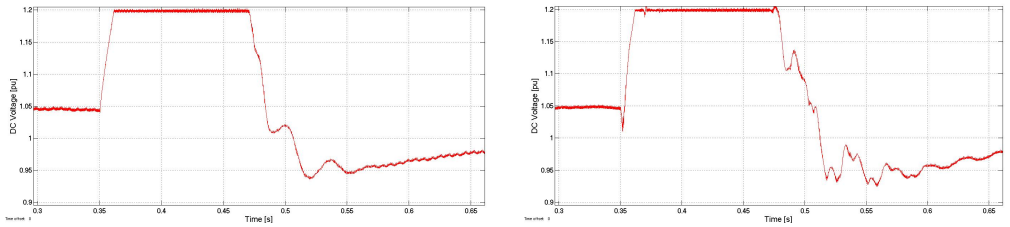

(a) Fault at Point B without NSCC (b) Fault at Point B with NSCC

Figure 71: WTG DC Voltage During a 3PG Fault

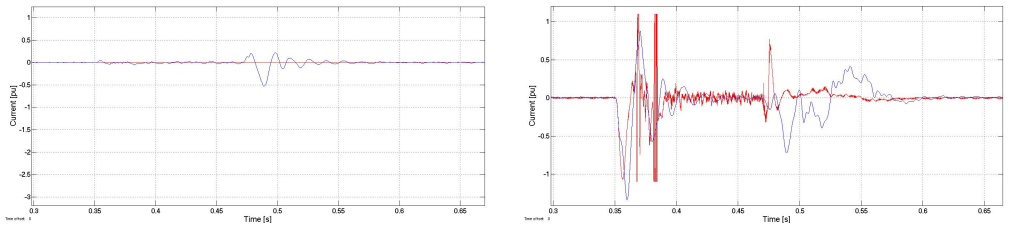

(a) Fault at Point B without NSCC (b) Fault at Point B with NSCC

Figure 72: D Axis Negative Sequence Current During a 3PG Fault

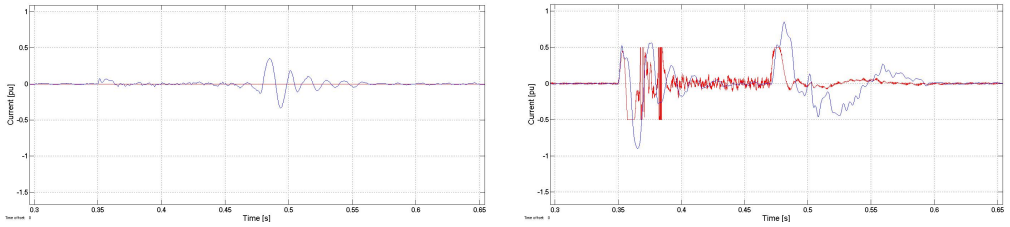

(a) Fault at Point B without NSCC (b) Fault at Point B with NSCC

Figure 73: Q Axis NSC During a 3PG Fault

E.5 Fault Effects During a DLG Fault with Zero NSC References

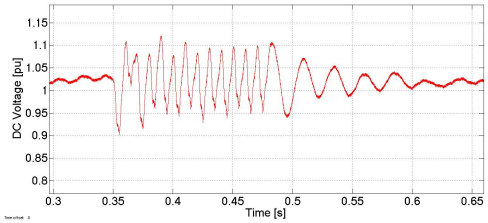

(a) Fault at Point B without NSCC

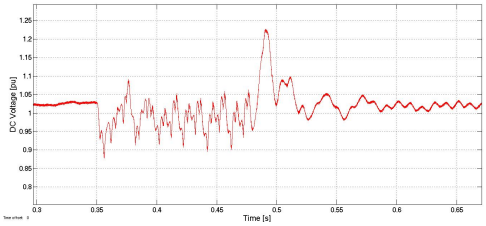

(b) Fault at Point B with NSCC

Figure 74: HVDC Link DC Voltage During a DLG Fault

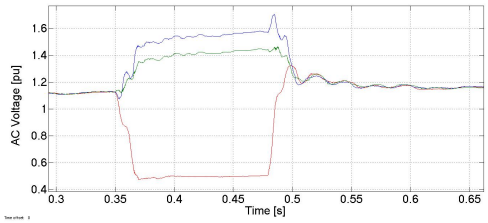

(a) Fault at Point B without NSCC

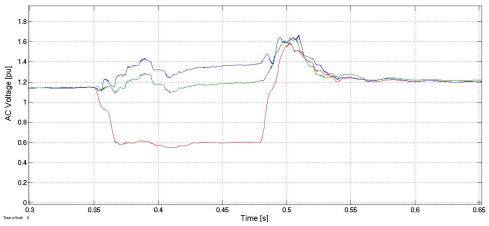

(b) Fault at Point B with NSCC

Figure 75: Offshore AC Grid Voltage During a DLG fault

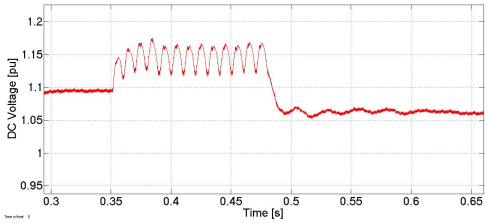

(a) Fault at Point B without NSCC

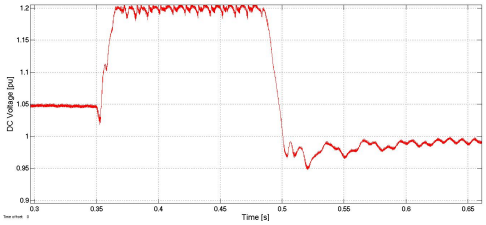

(b) Fault at Point B with NSCC

Figure 76: WTG DC Voltage During a DLG Fault

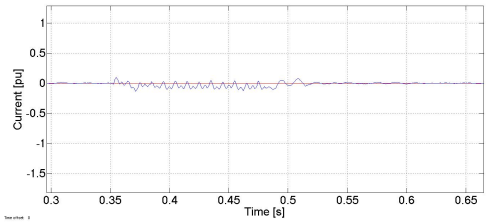

(a) Fault at Point B without NSCC

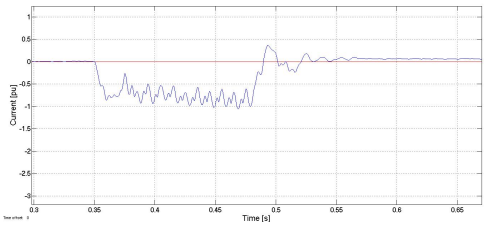

(b) Fault at Point B with NSCC

Figure 77: D Axis NSC During a DLG Fault

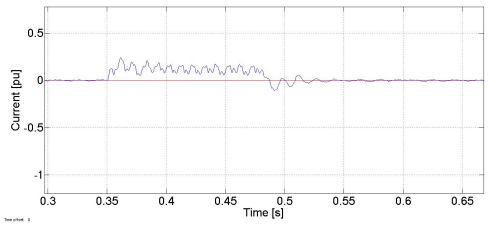

(a) Fault at Point B without NSCC

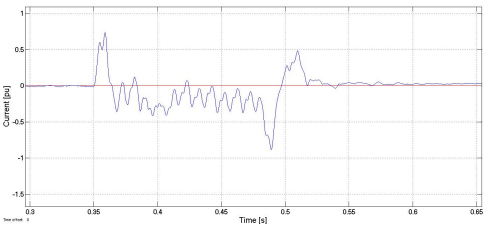

(b) Fault at Point B with NSCC

Figure 78: Q Axis NSC During a DLG Fault

F The SIMULINK Model

This section presents an overview over the SIMULINK model.

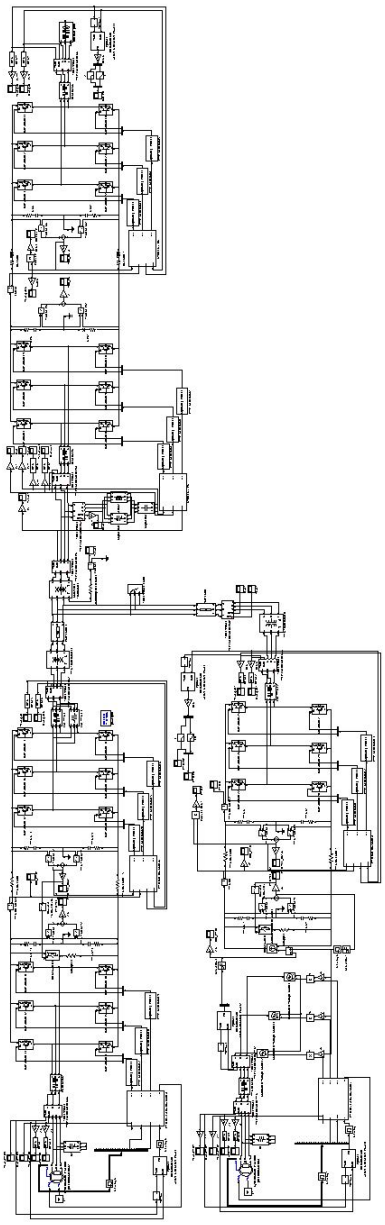

Figure 79: Complete SIMULINK Model

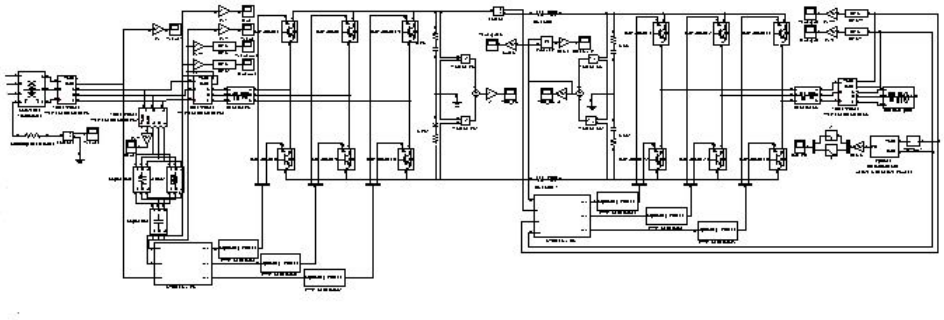

Figure 80: HVDC Link

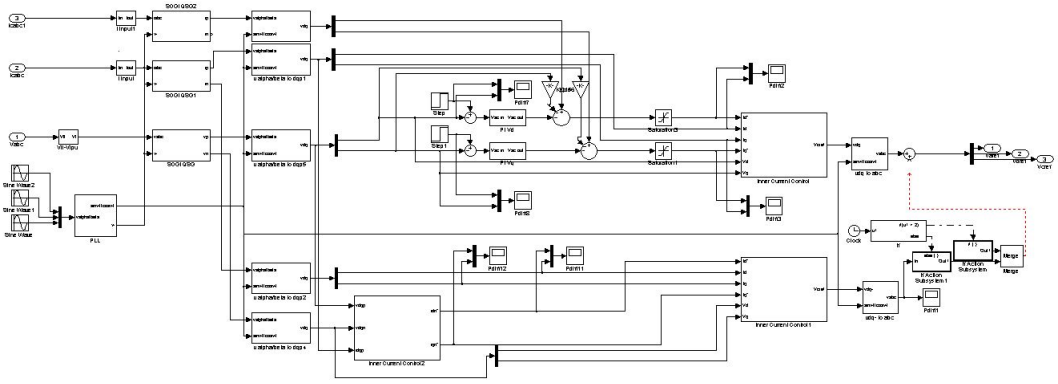

Figure 81: HVDC Link PS Converter Control System

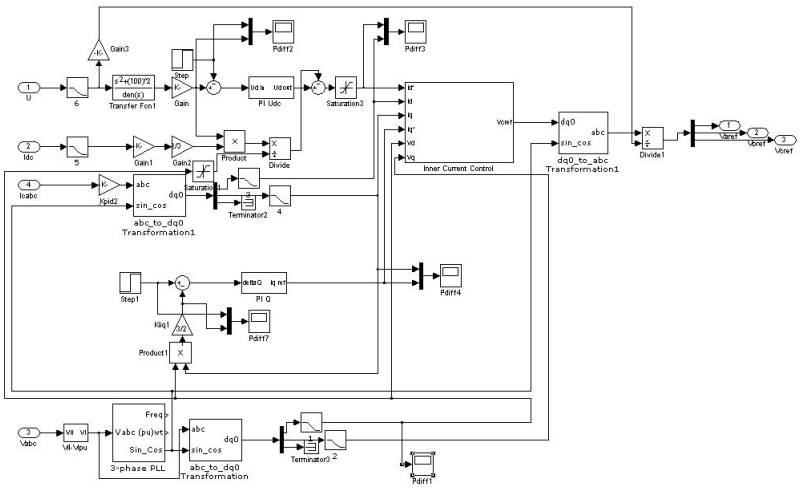

Figure 82: HVDC Link GS Converter Control System

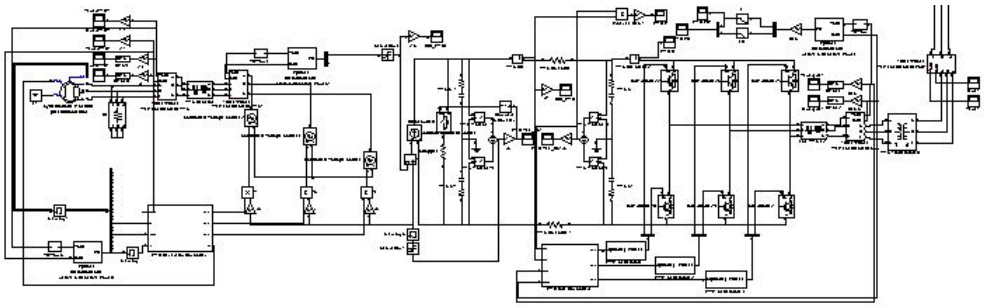

Figure 83: Wind Turbine Generator

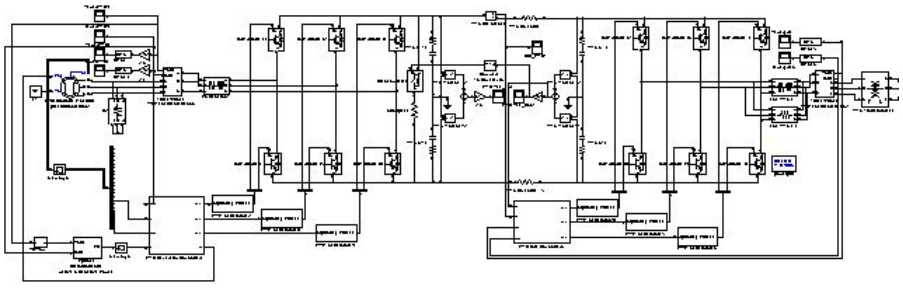

Figure 84: NOWITECH Reference Turbine

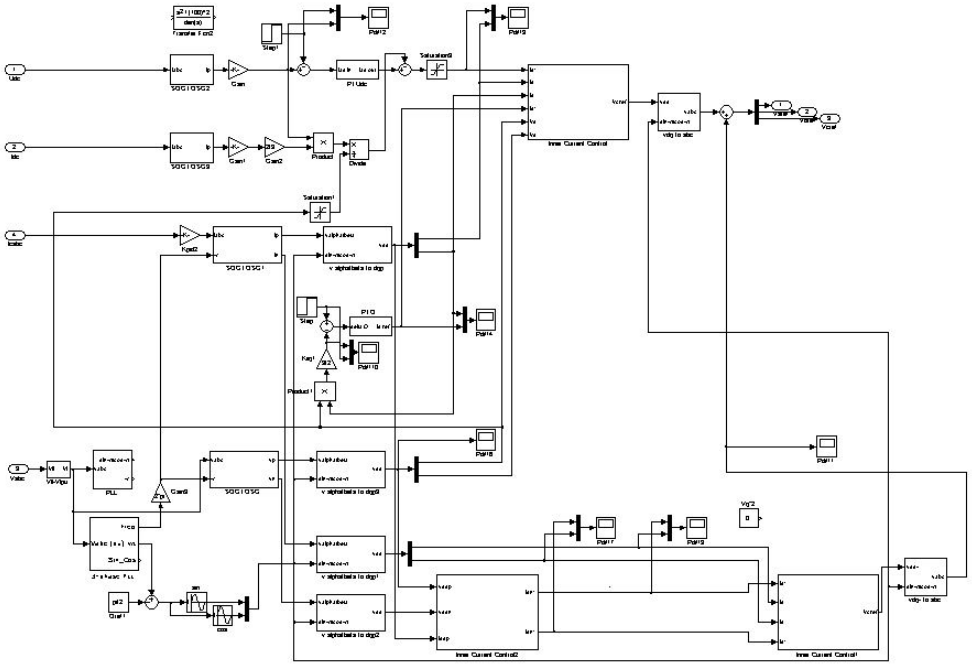

Figure 85: WTG PS Control System

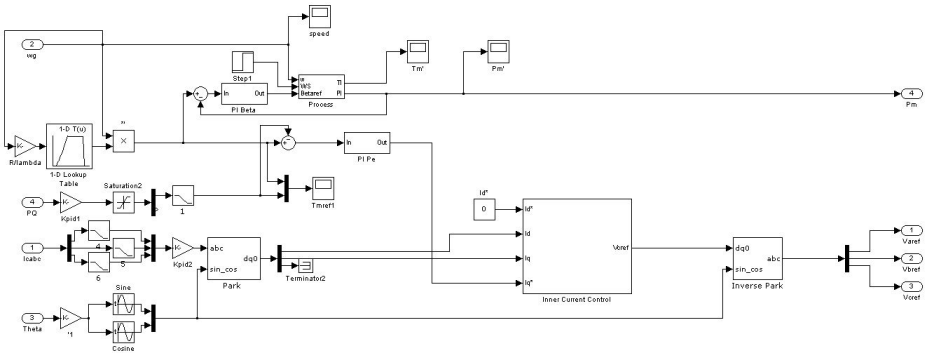

Figure 86: WTG TS Control System

References

[1] Global Wind Energy Council *Annual Market Update*. 2011.

[2] Paola Bresesti, Wil L. Kling, Ralph L. Hendriks and Riccardo Vailati, *HVDC Connection of Offshore Wind Farms to the Transmission System*. IEEE, 2007.

[3] ABB AB, *ABB HVDC Information Brochure: POW-0038 rev. 6*. 2010.

[4] Nowitech Project *http://www.sintef.no/projectweb/nowitech/*. 11.06.13.

[5] Nowitech Project Internal Data

[6] Sanjay K. Chaudary, *Control and Protection of Wind Power Plants with VSC-HVDC Connection*. 2011.

[7] Temesgen Mulugeta Haileselassie, *Control of Multi-terminal VSC-HVDC Systems*. 2008.

[8] Personal Correspondence with Jon Are Wold Suul

[9] Atle Rygg Årdal, *Feasibility Studies on Integrating Offshore Wind Power with Oil Platforms*. 2011.

[10] Hilde Evensen Liseth, *Dynamic Modeling of a Wind Turbine System*. 2011.

[11] Yan Wang, Shu-zhen Zhao, Cheng Huang-fu, Jiang-jun Ruan, Qing-da Meng and Jia-qi Zhao, *A Dynamic Model and Control Strategy for the Voltage Source Converter Based HVDC Transmission System under Fault AC Conditions*. 2009.

[12] Pedro Rodriguez, Adrian V. Timbus, Remus Teodorescu, Marco Liserre and Frede Blaabjerg, *Flexible Active Power Control of Distributed Power Generation Systems During Grid Faults*. 2007.

[13] Fei Wang, Jorge L. Duarte and Marcel A. M. Hendrix, *Pliant Active and Reactive Power Control for Grid-Interactivev Converters Under Unbalanced Voltage Dips*. 2011.

[14] S.K. Chaudary, R. Teodorescu, P. Rodrigueq, P.C. Kjaer, *Control and Operation of Wind Turbine Converters during Faults in an Offshore Wind Power Plant Grid with VSC-HVDC Connection*. 2011.

[15] Wind Power Monthly, Wind Power News Site, *http://www.windpowermonthly.com/go/windalert/article/1129734/?DCMP=EMC-CONWindpowerWeekly*. 18.12.12.

[16] Taylor & Francis Group, Electric Power Engineering Handbook Manuel Reta-Hernàndez, Chapter 13: Transmission Line Parameters *http://www.unioviedo.es/pcasielles/uploads/proyectantes/cosas_lineas.pdf*. LLC, 2006.

[17] ABB Submarine Cable System sheet *http://www05.abb.com/global/scot/scot245.nsf/veritydisplay/2fb0094306e48975c125777c00334767/£file/XLPE%20Submarine%20Cable%20Systems%202GM5007%20rev%205.pdf*. 11.06.13

[18] MathWorks, Matlab and SIMULINK producers, *http://www.mathworks.se/help/physmod/powersys/ref/pll.html*. 11.06.13.

[19] Imperial College London Lecture Slides, Lecture 9: Poles, Zeros and Filters. *http://www.ee.ic.ac.uk/pcheung/teaching/ee2_signals/Lecture%209%20-%20Poles%20Zeros%20&%20Filters.pdf*. 11.06.13.

[20] Henrik Kirkeby, *AC Faults in HVDC-VSC Connected Offshore Wind Farms with Full Scale Wind Turbine Generator VSCs with Different AC System Grounding*. 2012.

[21] S. M. Muyeen *Wind Energy Conversion Systems: Technology and Trends*. Lie Xu and Liangzhong Yao *Chapter 17: Fault Ride-Through of HVDC Connected Large Offshore Wind Farms* Springer, 2011.

[22] Chandra Bajracharya, Marta Molinas, Jon Are Suul and Tore M. Undeland, *Understanding of tuning techniques of converter controllers for VSC-HVDC*. 2008.

[23] Yan Wang, Shu-zhen Zhao, Cheng Huang-fu, Jiang-jun Ruan, Qing-da Meng and Jia-qi Zhao, *VSC Transmission Operating Under Unbalanced AC Conditions - Analysis and Control Design*. 2005.

[24] Cuiqing Du, Ambra Sannimo and Math H.J. Bollen, *Analysis of response of VSC-based HVDC to unbalanced faults with different control system*. 2005.

[25] Lie Xu, Bjarne R. Andersen and Philip Cartwright *VSC Transmission Operating Under Unbalanced AC Conditions - Analysis and Control Design* 2005.

[26] MathWorks, Matlab and SIMULINK producers, *http://www.mathworks.se/support/solutions/en/data/1-16V6S/*. 11.06.13.